

Effects of Family Non-universal Z' Model in the angular observables of $B \rightarrow (\rho, a_1)\mu^+\mu^-$ decays

Nimra Farooq,^{*} Marwah Zaki,[†] M. Ali Paracha,[‡] and Faisal Munir Bhutta[§]

Department of Physics, School of Natural Sciences, National University of Sciences and Technology, H-12, Islamabad, 44000, Pakistan

July 2, 2024

Abstract

We present the angular distribution of the four-fold $B \rightarrow \rho(\rightarrow \pi\pi)\mu^+\mu^-$ and $B \rightarrow a_1(\rightarrow \rho_{\parallel,\perp}\pi)\mu^+\mu^-$ decays both in the Standard Model and the family non-universal Z' model. At the quark level, these decays are governed by the $b \rightarrow d\mu^+\mu^-$ transition. Along with different angular observables, we also give predictions of differential branching ratios, forward-backward asymmetry, longitudinal polarization fraction of ρ , and a_1 mesons. Our analysis shows that the signatures of family non-universal Z' model are more distinct in the observables associated with the $B \rightarrow \rho(\rightarrow \pi\pi)\mu^+\mu^-$ decay, compared to that of the $B \rightarrow a_1(\rightarrow \rho_{\parallel,\perp}\pi)\mu^+\mu^-$ decay. Future measurements of the predicted angular observables, both at current and future high energy colliders, will add to the useful complementary data required to clarify the structure of the family non-universal Z' model in $|\Delta b|=|\Delta d|=1$ processes.

1 Introduction

Flavor physics plays a pivotal role not only in testing the Standard Model (SM) parameters but also in tracing out the signatures of New Physics (NP). Much of the efforts in this area focus on the detailed study of B meson decays as they are rich in phenomenology. Furthermore, from the NP point of view the rare decays of B meson, in particular the decays induced by flavor changing neutral current (FCNC) transitions $b \rightarrow q$ with $q = d, s$ are of great interest, as these decays are loop suppressed and only allowed via GIM mechanism in the SM [1]. Specifically, the observables involved in the rare radiative $b \rightarrow q\gamma$ and the rare semileptonic $b \rightarrow q\ell^+\ell^-$ decays allow to explore the structure of NP. Semileptonic decays which involve $b \rightarrow s$ current have been analyzed rigorously over the past many years and they have shown discrepancies from the SM predictions both in the lepton flavor-dependent (LFD) observables and the lepton flavor-independent observables defined as lepton flavor universality (LFU) ratios.

Among LFD ($b \rightarrow s\mu\mu$) observables, deviations are observed from the SM predictions, in the branching fractions of $B \rightarrow K\mu^+\mu^-$ [2], $B \rightarrow K^*\mu^+\mu^-$ [2-4], and $B_s \rightarrow \phi\mu^+\mu^-$ [5,6] decays.

^{*}nimrafarooq_1995@hotmail.com

[†]marwahiiui@gmail.com

[‡]aliparacha@sns.nust.edu.pk

[§]faisal.munir@sns.nust.edu.pk

The observed branching fractions suggest lower values as compared to their SM predictions. Also, in the $B^0 \rightarrow K^{*0} \mu^+ \mu^-$ decay, the angular observable, P'_5 , has shown mismatch from the SM values [7, 8]. Interestingly, global fits predict the NP effects being present in the LFD observables, involving $b \rightarrow s \mu \mu$ transition. Following it, NP effects in different complementary decay modes, driven by the same quark level transition $b \rightarrow s \mu \mu$, such as $B \rightarrow K_1 \mu^+ \mu^-$ [9–12], $B \rightarrow K_2^* \mu^+ \mu^-$ [13, 14], $B_s \rightarrow f_2' \mu^+ \mu^-$ [14, 15], and $B_c \rightarrow D_s^{(*)} \mu^+ \mu^-$ [16–19] have been investigated both in model-independent approach and the specific NP models.

LFU ratios in $b \rightarrow s$ sector have been measured by LHCb collaboration [20–22], defined as $R_{K^{(*)}} = \frac{\mathcal{B}(B \rightarrow K^{(*)} \mu^+ \mu^-)}{\mathcal{B}(B \rightarrow K^{(*)} e^+ e^-)}$, in different q^2 bins, and their analysis showed a 3σ deviation from the SM prediction. A similar analysis has been done by BELLE collaboration [23, 24], for the same ratios $R_{K^{(*)}}$ in the $q^2 \in (1 - 6)$ GeV² bin and it shows consistency with the SM predictions but with large experimental uncertainties. Furthermore, the recent measurements of the ratios $R_{K^{(*)}}$ in the low and central q^2 region of the spectrum by LHCb collaboration [25, 26], have shown an agreement with the SM predictions.

Apart from the LFU violation in $R_{K^{(*)}}$, LFU violation has also been studied in flavor changing charged current (FCCC) semileptonic $B \rightarrow D^{(*)} \ell \nu_\ell$ decay mode via the ratios $R_{D^{(*)}} = \frac{\mathcal{B}(B \rightarrow D^{(*)} \tau^+ \nu_\tau)}{\mathcal{B}(B \rightarrow D^{(*)} \ell \nu_\ell)}$ with ($\ell = e, \mu$) [27–30]. However the recent analysis of R_{D^*} and R_D by LHCb [31] and Belle collaboration [32], shows a good agreement with the SM predictions. To draw any conclusion regarding the status of NP, one must exploit the other sectors.

In this work, we consider FCNC processes governed by $b \rightarrow d \ell^+ \ell^-$ transition, as these modes are CKM suppressed compared to that of $b \rightarrow s \ell^+ \ell^-$ transitions. The typical branching ratios that belong to $b \rightarrow d \ell^+ \ell^-$ processes are of order 10^{-8} , and hence the measurements of these modes are considered to be challenging. Up to now only the branching ratios of rare $b \rightarrow d \mu^+ \mu^-$ and $b \rightarrow d \gamma$ decays have been measured, and the observed decay modes are (i) $B^+ \rightarrow \pi^+ \mu^+ \mu^-$ [33] (ii) $B^0 \rightarrow \mu^+ \mu^-$ [34] (iii) $B_s^0 \rightarrow K^{*0} \mu^+ \mu^-$ [35] (iv) $B \rightarrow X_d \gamma$ [36, 37]. In literature, researchers use the data set to extract information on NP Wilson coefficients from the global fit analysis, see Refs. [38–41]. Furthermore, the experimental data can be used to extract the information on the Wilson coefficients of different NP models such as family non-universal Z' Model [42, 43], supersymmetric models [44] and Two Higgs doublet Models [45].

The goal of our study is to use the family non-universal Z' effective Hamiltonian and perform the four-fold angular analysis of $B \rightarrow \rho(\rightarrow \pi\pi) \mu \mu$ and $B \rightarrow a_1(\rightarrow \rho_{\parallel, \perp} \pi) \mu \mu$ decays. For $B \rightarrow \rho$ decay we use the fit results for simplified series expansion (SSE) coefficients in the fit to Light cone sum rules (LCSR) form factors [46], and for the $B \rightarrow a_1$ decay we use the perturbative QCD (pQCD) form factors [47]. Both the decays are analyzed in the low q^2 region of the spectrum. For the decay channel $\rho \rightarrow \pi\pi$ the probability is 100%, while for the decays $a_1 \rightarrow \rho_{\parallel} \pi$, and $a_1 \rightarrow \rho_{\perp} \pi$ the probability is and 17% and 43%, respectively. In our study we choose the values of Wilson coefficients from [43] and give the predictions of different physical observables such as differential branching fractions, forward-backward asymmetry, longitudinal helicity fraction of ρ and a_1 mesons, and the individual normalized angular observables within the SM and the two scenarios of the family non-universal Z' model.

The organization of this paper is as follows: In section 2, we present the theoretical framework which includes effective Hamiltonian of the family non-universal Z' model for $b \rightarrow d \mu^+ \mu^-$ transition, where the basis operators remain the same as that of the SM. We then express the matrix elements for $B \rightarrow \rho \mu^+ \mu^-$ and $B \rightarrow a_1 \mu^+ \mu^-$ decays in terms of form factors. Furthermore, using the helicity formalism, we derive the four-fold angular decay distribution of $B \rightarrow \rho(\rightarrow \pi\pi) \mu \mu$, and $B \rightarrow a_1(\rightarrow \rho_{\parallel, \perp} \pi) \mu \mu$ decays, which contains the angular coefficients given

in terms of the helicity amplitudes. These angular coefficients are then used to construct various physical observables along with the normalized angular coefficients. In section 3, we present the numerical analysis of the physical observables in the SM and the family non-universal Z' model, and finally, section 4, summarizes our work.

2 Theoretical Framework

In this section, we provide the effective electroweak (EW) Hamiltonian approach [48, 49], where the SM heavy degrees of freedom such as W^\pm , Z^0 gauge bosons and the top quark are integrated out. The effective Hamiltonian is then used to calculate the full angular distribution of $B \rightarrow \rho(770)(\rightarrow \pi\pi)\mu^+\mu^-$ and $B \rightarrow a_1(1260)(\rightarrow \rho_{\parallel,\perp}\pi)\mu^+\mu^-$ decays. Using the form of four-fold angular distribution, we extract the q^2 dependent angular coefficients, which further will be used to analyze the signatures of the family non-universal Z' model.

2.1 Highlights of the Family Non-universal Z' Model

A family non-universal Z' gauge boson can naturally be derived in many extensions of the SM. The simplest way to incorporate the Z' gauge boson is by incorporating extra $U'(1)$ gauge symmetry. The model was formulated by Langacker and Plümacher [50]. One of the features of this model is that FCNC transitions could be induced at tree level, due to the non-diagonal chiral coupling matrix. The signatures of Z' gauge boson arise in two different ways.

- (i) By introducing new Wilson coefficients only and the basis of operators remains the same as that of SM.
- (ii) In other approach, new Wilson coefficients and new operators are added to the SM effective Hamiltonian.

In this work, we will analyze the family non-universal Z' model using the above mentioned B meson decays, and the NP in this model arises due to the modification of the Wilson coefficients C_9^{eff} and C_{10} , the structure of the operators remains the same as that of SM. The Wilson coefficients can get modified due to the off-diagonal couplings of quarks as well as leptons with Z' gauge boson. The current due to extra $U'(1)$ gauge symmetry in the SM eigenstate basis can be written as [50, 51]

$$J_\mu = \sum_{i,j} \bar{\psi}_i \gamma_\mu [\epsilon_{\psi_{Lij}} P_L + \epsilon_{\psi_{Rij}} P_R] \psi_j, \quad (1)$$

where the summation runs overall quarks and leptons field ψ_{ij} , $P_{R,L} = \frac{1}{2}(1 \pm \gamma^5)$ are the right-handed and left-handed projectors, and $\epsilon_{\psi_{R,L}}$ indicates the chiral couplings of the new gauge boson.

As already discussed, in the family non-universal Z' model, FCNC transition arises at the tree level if the chiral coupling matrices $\epsilon_{\psi_{R,L}}$ are non-diagonal, however if the couplings of Z' gauge bosons are diagonal but non-universal, flavor-changing couplings are generated by fermion mixing. The fermion Yukawa matrix h_ψ can be diagonalized in the weak eigenstate basis through CKM unitary matrices $V_{R,L}^\psi$ and can be expressed as,

$$h_{\psi,diag} = V_R^\psi h_\psi V_L^{\dagger\psi}. \quad (2)$$

Hence, the chiral Z' couplings in the fermion mass eigenstates can be expressed as [51]

$$B_{ij}^{\psi_L} = (V_L^\psi \epsilon_{\psi_L} V_L^{\dagger\psi})_{ij}, \quad B_{ij}^{\psi_R} = (V_R^\psi \epsilon_{\psi_R} V_R^{\dagger\psi})_{ij}. \quad (3)$$

In Eq. (3), the non-vanishing quark coupling matrices $B_{ij}^{\psi_{L,R}}$ represent the signature of the NP, and also two decades ago it was shown that the flavor non-universal Z' model can be used to improve the precision of electroweak data [52].

At quark level the decay $B \rightarrow M\mu^+\mu^-$ ($M = \rho(770), a_1(1260)$) modes are governed by $b \rightarrow d$ transitions, hence the FCNC Lagrangian due to Z' model can be written as [43]

$$\mathcal{L}_{\text{FCNC}}^{Z'} = -g'(B_{db}^L \bar{d}_L \gamma_\mu b_L + B_{db}^R \bar{d}_R \gamma_\mu b_R) Z'^\mu + h.c., \quad (4)$$

where g' is the gauge coupling associated with $U'(1)$ gauge group.

2.2 Effective Hamiltonian for $b \rightarrow d\mu^+\mu^-$ Transition in the SM and the Z' Model

The signatures of Z' gauge boson can also be analyzed through the decay modes of B mesons within the framework of SM low energy effective field theory. As mentioned earlier that in this framework, the heavy degrees of freedom including the new particles are integrated out (Wilson coefficients), and the effective Hamiltonian appears in terms of four Fermi operators as well as the Wilson coefficients.

The effective Hamiltonian for modes $B \rightarrow M\mu^+\mu^-$ ($M = \rho(770), a_1(1260)$) in the SM can be written as,

$$H_{\text{eff}}^{\text{SM}} = -\frac{4G_F\alpha}{\sqrt{2}} V_{tb} V_{td}^* \left[\sum_{i=1}^{10} C_i O_i - \lambda_u \{C_1 [O_1^u - O_1] + C_2 [O_2^u - O_2]\} \right], \quad (5)$$

where G_F is the Fermi coupling constant, V_{ij} , and $\lambda_u = \frac{V_{ub}V_{ud}^*}{V_{tb}V_{td}^*}$, are the corresponding CKM factors and their ratios, respectively. The explicit form of the four fermion operators that contribute to the said process in the SM can be written as,

$$\begin{aligned} O_{7\gamma} &= \frac{e}{16\pi^2} m_b (\bar{d}\sigma_{\mu\nu} P_R b) F^{\mu\nu}, \\ O_9 &= \frac{e^2}{16\pi^2} (\bar{d}\gamma_\mu P_L b) (\bar{\ell}\gamma^\mu \ell), \\ O_{10} &= \frac{e^2}{16\pi^2} (\bar{d}\gamma_\mu P_L b) (\bar{\ell}\gamma^\mu \gamma_5 \ell), \end{aligned} \quad (6)$$

where $F^{\mu\nu}$ are the electromagnetic field strength tensor, e is an electromagnetic coupling constant and m_b appears in the electromagnetic dipole operator expression is the running b quark mass in $\overline{\text{MS}}$ scheme.

In Eq. (5), $C_i(\mu)$ represents the Wilson coefficients at the energy scale μ . The form of the $C_7^{\text{eff}}(q^2)$ and $C_9^{\text{eff}}(q^2)$ Wilson coefficients [39, 53–57], that contain the factorizable contributions from current-current, QCD penguins and chromomagnetic dipole operators $O_{1-6,8}$ are given in appendix A.

At the quark level the decays $B \rightarrow M\mu^+\mu^-$ are governed by $b \rightarrow d\mu^+\mu^-$ transition and in the framework of SM its amplitude can be written as,

$$\begin{aligned} \mathcal{M}^{\text{SM}}(b \rightarrow d\mu^+\mu^-) &= \frac{G_F\alpha V_{tb}V_{td}^*}{2\sqrt{2}\pi} \left\{ C_9^{\text{eff}} \langle M(k, \epsilon) | \bar{d}\gamma^\mu (1 - \gamma^5) b | B(p) \rangle \bar{\ell}\gamma_\mu \ell \right. \\ &+ C_{10}^{\text{SM}} \langle M(k, \epsilon) | \bar{d}\gamma^\mu (1 - \gamma^5) b | B(p) \rangle \bar{\ell}\gamma_\mu \gamma_5 \ell \\ &\left. - \frac{2m_b}{q^2} C_7^{\text{eff}} \langle M(k, \epsilon) | \bar{d}i\sigma^{\mu\nu} q_\nu (1 + \gamma^5) b | B(p) \rangle \bar{\ell}\gamma_\mu \ell \right\}, \end{aligned} \quad (7)$$

As discussed above that in the family non-universal Z' model, the FCNC transition arises at the tree level, hence by ignoring the $Z - Z'$ mixing and assuming that the couplings of right-handed quark flavors with Z' boson are diagonal [58–60], the effective Hamiltonian for $b \rightarrow d\mu^+\mu^-$ transition in the family non-universal Z' model can be straightforwardly written as,

$$\mathcal{H}_{\text{eff}}^{Z'} = -\frac{2G_F}{\sqrt{2}}V_{tb}V_{td}^* \left[-\frac{B_{db}^L B_{\ell\ell}^L}{V_{tb}V_{td}^*} (\bar{d}b)_{V-A} (\bar{\ell}\ell)_{V-A} - \frac{B_{db}^L B_{\ell\ell}^R}{V_{tb}V_{td}^*} (\bar{d}b)_{V-A} (\bar{\ell}\ell)_{V+A} \right], \quad (8)$$

where $B_{db}^L = |B_{db}^L|e^{-i\phi_{db}}$ represents the left-handed coupling of quarks with Z' gauge boson and ϕ_{db} is the new CP-violating phase which is not present in the SM. In condensed notation, one can write Eq. (8) as

$$\mathcal{H}_{\text{eff}}^{Z'} = -\frac{4G_F}{\sqrt{2}}V_{tb}V_{td}^* \left[\Lambda_{db} C_9^{Z'} O_9 + \Lambda_{db} C_{10}^{Z'} O_{10} \right], \quad (9)$$

where

$$\Lambda_{db} = \frac{4\pi e^{-i\phi_{db}}}{\alpha V_{tb}V_{td}^*}, \quad (10)$$

$$C_9^{Z'} = |B_{db}^L| S_{LR}; \quad C_{10}^{Z'} = |B_{db}^L| D_{LR}, \quad (11)$$

and

$$\begin{aligned} S_{LR} &= B_{\ell\ell}^L + B_{\ell\ell}^R, \\ D_{LR} &= B_{\ell\ell}^L - B_{\ell\ell}^R. \end{aligned} \quad (12)$$

In Eq. (12), S_{LR} and D_{LR} constitutes the couplings of new Z' gauge boson with left and right-handed leptons. The total amplitude for the decay $B \rightarrow M\mu^+\mu^-$ in terms of SM and in Z' model can be written as,

$$\begin{aligned} \mathcal{M}^{\text{tot}}(b \rightarrow d\ell^+\ell^-) &= \frac{G_F\alpha V_{tb}V_{td}^*}{2\sqrt{2}\pi} \left\{ C_9^{\text{tot}} \langle M(k, \epsilon) | \bar{d}\gamma^\mu (1 - \gamma^5) b | B(p) \rangle \bar{\ell}\gamma_\mu \ell \right. \\ &+ C_{10}^{\text{tot}} \langle M(k, \epsilon) | \bar{d}\gamma^\mu (1 - \gamma^5) b | B(p) \rangle \bar{\ell}\gamma_\mu \gamma_5 \ell \\ &\left. - \frac{2m_b}{q^2} C_7^{\text{eff}} \langle M(k, \epsilon) | \bar{d}i\sigma^{\mu\nu} q_\nu (1 + \gamma^5) b | B(p) \rangle \bar{\ell}\gamma_\mu \ell \right\}, \quad (13) \end{aligned}$$

where in Eq. (13)

$$\mathcal{M}^{\text{tot}} = \mathcal{M}^{\text{SM}} + \mathcal{M}^{\text{ZP}}, \quad (14)$$

and

$$\begin{aligned} C_9^{\text{tot}} &= C_9^{\text{eff}} + \Lambda_{db} C_9^{Z'}, \\ C_{10}^{\text{tot}} &= C_{10}^{\text{SM}} + \Lambda_{db} C_{10}^{Z'}. \end{aligned} \quad (15)$$

The amplitude for the decays $B \rightarrow M\ell^+\ell^-$ in the framework of SM and in the family non-universal Z' model can also be written as,

$$\mathcal{M}^{\text{tot}}(B \rightarrow M\ell^+\ell^-) = \frac{G_F\alpha}{2\sqrt{2}\pi} V_{tb}V_{td}^* \left\{ T_\mu^{1,M}(\bar{\ell}\gamma^\mu \ell) + T_\mu^{2,M}(\bar{\ell}\gamma^\mu \gamma_5 \ell) \right\}, \quad (16)$$

where

$$T_\mu^{1,M} = C_9^{\text{tot}} \langle M(k, \epsilon) | \bar{s}\gamma_\mu (1 - \gamma_5) b | B(p) \rangle - \frac{2m_b}{q^2} C_7^{\text{eff}} \langle M(k, \epsilon) | \bar{s}i\sigma_{\mu\nu} q^\nu (1 + \gamma_5) b | B(p) \rangle, \quad (17)$$

$$T_\mu^{2,M} = C_{10}^{\text{tot}} \langle M(k, \epsilon) | \bar{s}\gamma_\mu (1 - \gamma_5) b | B(p) \rangle, \quad (18)$$

where $T_\mu^{i,M}$, $i = (1, 2)$, contain the matrix elements of $B \rightarrow M$.

2.3 Matrix Elements of $B \rightarrow (\rho(770), a_1(1260))\mu^+\mu^-$ Decays

The form factors for $B \rightarrow \rho$ and $B \rightarrow a_1$ decays can be expressed in terms of Lorentz invariant form factors as,

$$\langle \rho(k, \bar{\epsilon}) | \bar{s}\gamma_\mu b | B(p) \rangle = \frac{2\epsilon_{\mu\nu\alpha\beta} \bar{\epsilon}^{*\nu} p^\alpha k^\beta V(q^2)}{m_B + m_\rho}, \quad (19)$$

$$\begin{aligned} \langle \rho(k, \bar{\epsilon}) | \bar{s}\gamma_\mu \gamma_5 b | B(p) \rangle &= i(m_B + m_\rho) g_{\mu\nu} \bar{\epsilon}^{*\nu} A_1(q^2) \\ &\quad - iP_\mu(\bar{\epsilon}^* \cdot q) \frac{A_2(q^2)}{(m_B + m_\rho)} \\ &\quad - i \frac{2m_\rho}{q^2} q_\mu(\bar{\epsilon}^* \cdot q) [A_3(q^2) - A_0(q^2)], \end{aligned} \quad (20)$$

where $P_\mu = p_\mu + k_\mu$, $q_\mu = p_\mu - k_\mu$, and with $A_3(0) = A_0(0)$. We have used $\epsilon_{0123} = +1$ convention throughout the study. The additional tensor form factors are expressed as,

$$\langle \rho(k, \bar{\epsilon}) | \bar{s}i\sigma_{\mu\nu} q^\nu b | B(p) \rangle = -2\epsilon_{\mu\nu\alpha\beta} \bar{\epsilon}^{*\nu} p^\alpha k^\beta T_1(q^2), \quad (21)$$

$$\begin{aligned} \langle \rho(k, \bar{\epsilon}) | \bar{s}i\sigma_{\mu\nu} q^\nu \gamma_5 b | B(p) \rangle &= i \left[(m_B^2 - m_\rho^2) g_{\mu\nu} \bar{\epsilon}^{*\nu} \right. \\ &\quad \left. - (\bar{\epsilon}^* \cdot q) P_\mu \right] T_2(q^2) + i(\bar{\epsilon}^* \cdot q) \\ &\quad \times \left[q_\mu - \frac{q^2}{m_B^2 - m_\rho^2} P_\mu \right] T_3(q^2). \end{aligned} \quad (22)$$

The relations between the form factors in [46], and the form factors given in above matrix elements are

$$\begin{aligned} A_{12}(q^2) &= \frac{(m_B + m_\rho)^2 (m_B^2 - m_\rho^2 - q^2) A_1(q^2) - \lambda A_2(q^2)}{16m_B m_\rho^2 (m_B + m_\rho)}, \\ T_{23}(q^2) &= \frac{(m_B^2 - m_\rho^2) (m_B^2 + 3m_\rho^2 - q^2) T_2(q^2) - \lambda T_3(q^2)}{8m_B m_\rho^2 (m_B - m_\rho)}. \end{aligned} \quad (23)$$

and

$$\begin{aligned} \langle a_1(k, \bar{\epsilon}) | V_\mu | B(p) \rangle &= -\bar{\epsilon}_\mu^* (m_B + m_{a_1}) V_1(q^2) + (p + k)_\mu (\bar{\epsilon}^* \cdot q) \frac{V_2(q^2)}{m_B + m_{a_1}} \\ &\quad + q_\mu (\bar{\epsilon}^* \cdot q) \frac{2m_{a_1}}{q^2} [V_3(q^2) - V_0(q^2)], \end{aligned} \quad (24)$$

$$\langle a_1(k, \bar{\epsilon}) | A_\mu | B(p) \rangle = \frac{2i\epsilon_{\mu\nu\alpha\beta} \bar{\epsilon}^{*\nu} p^\alpha k^\beta A(q^2)}{m_B + m_{a_1}}, \quad (25)$$

where $V^\mu = \bar{d}\gamma^\mu b$ and $A^\mu = \bar{d}\gamma^\mu \gamma_5 b$ are vector and axial vector currents, $\bar{\epsilon}^{*\nu}$ are polarization vectors of the axial vector meson. The relation for vector form factor $V_3(q^2)$ given in Eq. (24) can be written as

$$\begin{aligned} V_3(q^2) &= \frac{m_B + m_{a_1}}{2m_{a_1}} V_1(q^2) - \frac{m_B - m_{a_1}}{2m_{a_1}} V_2(q^2), \\ V_3(0) &= V_0(0). \end{aligned} \quad (26)$$

$$\begin{aligned} \langle a_1(k, \bar{\epsilon}) | \bar{d}i\sigma_{\mu\nu} q^\nu b | B(p) \rangle &= [(m_B^2 - m_{a_1}^2) \bar{\epsilon}_\mu^* - (\bar{\epsilon}^* \cdot q)(p + k)_\mu] T_2(q^2) \\ &\quad + (\bar{\epsilon}^* \cdot q) \left[q_\mu - \frac{q^2}{m_B^2 - m_{a_1}^2} (p + k)_\mu \right] T_3(q^2), \end{aligned} \quad (27)$$

$$\langle a_1(k, \bar{\epsilon}) | \bar{d}i\sigma_{\mu\nu} q^\nu \gamma_5 b | B(p) \rangle = 2i\epsilon_{\mu\nu\alpha\beta} \bar{\epsilon}^{*\nu} p^\alpha k^\beta T_1(q^2). \quad (28)$$

2.4 Helicity Formalism of $B \rightarrow (\rho(770), a_1(1260))\mu^+\mu^-$ Decays

To calculate the angular distribution of the four-fold $B \rightarrow \rho(\rightarrow \pi\pi)\mu^+\mu^-$ and $B \rightarrow a_1(\rightarrow \rho_{\parallel,\perp}\pi)\mu^+\mu^-$ decays, we use the helicity formalism and follow [61]. The kinematics of the four-fold decays under consideration are shown in Fig. 1. The completeness and orthogonality properties of helicity basis can read as follows,

$$\varepsilon^{*\alpha}(n)\varepsilon_\alpha(l) = g_{nl}, \quad \sum_{n,l=t,+,-,0} \varepsilon^{*\alpha}(n)\varepsilon^\beta(l)g_{nl} = g^{\alpha\beta}, \quad (29)$$

with $g_{nl} = \text{diag}(+, -, -, -)$. From the completeness relation given in Eq. (29), the contraction of leptonic tensors $L^{(k)\alpha\beta}$ and hadronic tensors $H_{\alpha\beta}^{ij} = T_\alpha^{i,M}\bar{T}_\beta^{j,M}$ ($i, j = 1, 2$), can be written as

$$L^{(k)\alpha\beta}H_{\alpha\beta}^{ij} = \sum_{n,n',l,l'} L_{nl}^{(k)}g_{nm'}g_{l'l''}H_{n'l''}^{ij}, \quad (30)$$

where the leptonic and hadronic tensors can be written in the helicity basis as follows

$$L_{nl}^{(k)} = \varepsilon^\alpha(n)\varepsilon^{*\beta}(l)L_{\alpha\beta}^{(k)}, \quad H_{nl}^{ij} = \varepsilon^{*\alpha}(n)\varepsilon^\beta(l)H_{\alpha\beta}^{ij}. \quad (31)$$

Both leptonic and hadronic tensors shown in Eq. (31), can be evaluated in two different frames of reference. The lepton tensor $L_{nl}^{(k)}$ is evaluated in the dimuon center of mass (CM) frame, and the hadronic tensor H_{nl}^{ij} is evaluated in the rest frame of B meson. For the above mentioned decays, one can write the hadronic tensor as follows,

$$\begin{aligned} H_{nl}^{ij} &= (\varepsilon^{*\alpha}(n)T_\alpha^{i,M}) \cdot (\overline{\varepsilon^{*\beta}(l)T_\beta^{j,M}}) \\ &= (\varepsilon^{*\alpha}(n)\bar{\epsilon}^{*\mu}(r)T_{\alpha,\mu}^{i,M}) \cdot (\overline{\varepsilon^{*\beta}(l)\bar{\epsilon}^{*\nu}(s)T_{\beta,\nu}^{j,M}})\delta_{rs} \equiv H_n^{i,M}\bar{H}_l^{j,M_l}. \end{aligned} \quad (32)$$

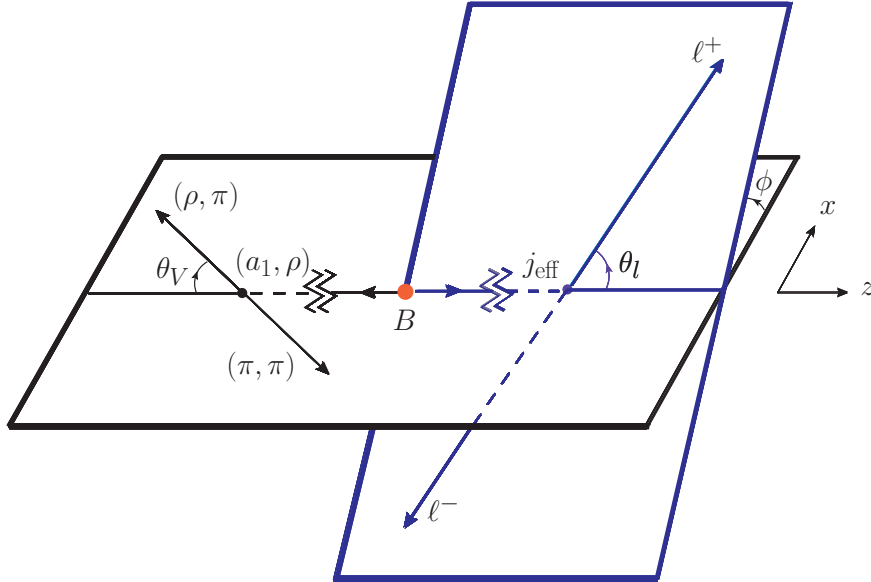


Figure 1: Kinematics of the $B \rightarrow \rho(\rightarrow \pi\pi)l^+l^-$, and $B \rightarrow a_1(\rightarrow \rho\pi)l^+l^-$ decays.

2.5 Helicity Amplitudes for $B \rightarrow \rho\mu^+\mu^-$ and $B \rightarrow a_1\mu^+\mu^-$ Decays

The explicit expressions of the helicity amplitudes for $B \rightarrow \rho$ and $B \rightarrow a_1$, are given as

$$\begin{aligned}
H_t^{1,\rho} &= -i\sqrt{\frac{\lambda}{q^2}}C_9^{\text{tot}}A_0(q^2), \\
H_t^{2,\rho} &= -i\sqrt{\frac{\lambda}{q^2}}C_{10}^{\text{tot}}A_0(q^2), \\
H_{\pm}^{1,\rho} &= -i(m_B^2 - m_\rho^2) \left[C_9^{\text{tot}} \frac{A_1(q^2)}{(m_B - m_\rho)} \right. \\
&\quad \left. + \frac{2m_b}{q^2}C_7^{\text{eff}}T_2(q^2) \right] \pm i\sqrt{\lambda} \left[C_9^{\text{tot}} \frac{V(q^2)}{(m_B + m_\rho)} + \frac{2m_b}{q^2}C_7^{\text{eff}}T_1(q^2) \right], \\
H_{\pm}^{2,\rho} &= -iC_{10}^{\text{tot}}(m_B + m_\rho)A_1(q^2) \pm i\sqrt{\lambda}C_{10}^{\text{tot}}\frac{V(q^2)}{(m_B + m_\rho)}, \\
H_0^{1,\rho} &= -\frac{8im_Bm_\rho}{\sqrt{q^2}} \left[C_9^{\text{tot}}A_{12}(q^2) + m_bC_7^{\text{eff}}\frac{T_{23}(q^2)}{m_B + m_\rho} \right], \\
H_0^{2,\rho} &= -\frac{8im_Bm_\rho}{\sqrt{q^2}} \left[C_{10}^{\text{tot}}A_{12}(q^2) \right]. \tag{33}
\end{aligned}$$

and

$$\begin{aligned}
H_t^{1,a_1} &= -\sqrt{\frac{\lambda}{q^2}}C_9^{\text{tot}}V_0(q^2), \\
H_t^{2,a_1} &= -\sqrt{\frac{\lambda}{q^2}}C_{10}^{\text{tot}}V_0(q^2), \\
H_{\pm}^{1,a_1} &= -(m_B^2 - m_{a_1}^2) \left[C_9^{\text{tot}} \frac{V_1(q^2)}{(m_B - m_{a_1})} + \frac{2m_b}{q^2}C_7^{\text{eff}}T_2(q^2) \right] \\
&\quad \pm \sqrt{\lambda} \left[C_9^{\text{tot}} \frac{A(q^2)}{(m_B + m_{a_1})} + \frac{2m_b}{q^2}C_7^{\text{eff}}T_1(q^2) \right], \\
H_{\pm}^{2,a_1} &= -C_{10}^{\text{tot}}(m_B + m_{a_1})V_1(q^2) \pm \sqrt{\lambda}C_{10}^{\text{tot}}\frac{A(q^2)}{(m_B + m_{a_1})}, \\
H_0^{1,a_1} &= -\frac{1}{2m_{a_1}\sqrt{q^2}} \left[C_9^{\text{tot}} \left\{ (m_B^2 - m_{a_1}^2 - q^2)(m_B + m_{a_1})V_1(q^2) \right. \right. \\
&\quad \left. \left. - \frac{\lambda}{m_B + m_{a_1}}V_2(q^2) \right\} + 2m_bC_7^{\text{eff}} \left\{ (m_B^2 + 3m_{a_1}^2 - q^2)T_2(q^2) - \frac{\lambda}{m_B^2 - m_{a_1}^2}T_3(q^2) \right\} \right], \\
H_0^{2,a_1} &= -\frac{1}{2m_{a_1}\sqrt{q^2}}C_{10}^{\text{tot}} \left[(m_B^2 - m_{a_1}^2 - q^2)(m_B + m_{a_1})V_1(q^2) - \frac{\lambda}{m_B + m_{a_1}}V_2(q^2) \right]. \tag{34}
\end{aligned}$$

2.6 Four fold distribution of $B \rightarrow \rho(\rightarrow \pi\pi)\mu^+\mu^-$ and $B \rightarrow a_1(\rightarrow \rho\pi)\mu^+\mu^-$ Decays

The four-fold decay distribution depends on the square of the dilepton invariant mass q^2 , angles θ_ℓ , θ_V and ϕ as shown in Fig. 1. For $B \rightarrow \rho$ decay mode, the four-fold distribution can be

written as,

$$\begin{aligned}
\frac{d^4\Gamma(B \rightarrow \rho(\rightarrow \pi\pi)\mu^+\mu^-)}{dq^2 d\cos\theta_l d\cos\theta_V d\phi} &= \frac{9}{32\pi}\mathcal{B}(\rho \rightarrow \pi\pi) \\
&\times \left[I_{1s}^\rho \sin^2\theta_V + I_{1c}^\rho \cos^2\theta_V \right. \\
&+ \left(I_{2s}^\rho \sin^2\theta_V + I_{2c}^\rho \cos^2\theta_V \right) \cos 2\theta_l \\
&+ \left(I_{6s}^\rho \sin^2\theta_V + I_{6c}^\rho \cos^2\theta_V \right) \cos\theta_l \\
&+ \left(I_3^\rho \cos 2\phi + I_9^\rho \sin 2\phi \right) \sin^2\theta_V \sin^2\theta_l \\
&+ \left(I_4^\rho \cos\phi + I_8^\rho \sin\phi \right) \sin 2\theta_V \sin 2\theta_l \\
&+ \left. \left(I_5^\rho \cos\phi + I_7^\rho \sin\phi \right) \sin 2\theta_V \sin\theta_l \right].
\end{aligned} \tag{35}$$

The explicit expressions of $I_{n\lambda}^\rho$ in terms of the helicity amplitudes are obtained as,

$$\begin{aligned}
I_{1s}^\rho &= \frac{(2 + \beta_l^2)}{2} N^2 (|H_+^1|^2 + |H_+^2|^2 + |H_-^1|^2 + |H_-^2|^2) \\
&+ \frac{4m_l^2}{q^2} N^2 (|H_+^1|^2 - |H_+^2|^2 + |H_-^1|^2 - |H_-^2|^2),
\end{aligned} \tag{36}$$

$$I_{1c}^\rho = 2N^2 (|H_0^1|^2 + |H_0^2|^2) + \frac{8m_l^2}{q^2} N^2 (|H_0^1|^2 - |H_0^2|^2 + 2|H_t^2|^2), \tag{37}$$

$$I_{2s}^\rho = \frac{\beta_l^2}{2} N^2 (|H_+^1|^2 + |H_+^2|^2 + |H_-^1|^2 + |H_-^2|^2), \tag{38}$$

$$I_{2c}^\rho = -2\beta_l^2 N^2 (|H_0^1|^2 + |H_0^2|^2), \tag{39}$$

$$I_3^\rho = -2\beta_l^2 N^2 \left[\mathcal{R}e (H_+^1 H_-^{1*} + H_+^2 H_-^{2*}) \right], \tag{40}$$

$$I_4^\rho = \beta_l^2 N^2 \left[\mathcal{R}e (H_+^1 H_0^{1*} + H_-^1 H_0^{1*}) + \mathcal{R}e (H_+^2 H_0^{2*} + H_-^2 H_0^{2*}) \right], \tag{41}$$

$$I_5^\rho = -2\beta_l N^2 \left[\mathcal{R}e (H_+^1 H_0^{2*} - H_-^1 H_0^{2*}) + \mathcal{R}e (H_+^2 H_0^{1*} - H_-^2 H_0^{1*}) \right], \tag{42}$$

$$I_{6s}^\rho = -4\beta_l N^2 \left[\mathcal{R}e (H_+^1 H_+^{2*} - H_-^1 H_-^{2*}) \right], \tag{43}$$

$$I_{6c}^\rho = 0, \tag{44}$$

$$I_7^\rho = -2\beta_l N^2 \left[\mathcal{I}m (H_0^1 H_+^{2*} + H_0^1 H_-^{2*}) + \mathcal{I}m (H_0^2 H_+^{1*} + H_0^2 H_-^{1*}) \right], \tag{45}$$

$$I_8^\rho = \beta_l^2 N^2 \left[\mathcal{I}m (H_0^1 H_+^{1*} - H_0^1 H_-^{1*}) + \mathcal{I}m (H_0^2 H_+^{2*} - H_0^2 H_-^{2*}) \right], \tag{46}$$

$$I_9^\rho = 2\beta_l^2 N^2 \left[\mathcal{I}m (H_+^1 H_-^{1*} + H_+^2 H_-^{2*}) \right], \tag{47}$$

For the decay $B \rightarrow a_1 (\rightarrow \rho_{\parallel(\perp)}\pi)\mu^+\mu^-$ the four fold distribution can be written as,

$$\begin{aligned}
\frac{d^4\Gamma (B \rightarrow a_1 (\rightarrow \rho_{\parallel(\perp)}\pi)\mu^+\mu^-)}{dq^2 d\cos\theta_l d\cos\theta_V d\phi} &= \frac{9}{32\pi}\mathcal{B}(a_1 \rightarrow \rho_{\parallel(\perp)}\pi) \\
&\times \left[I_{1s,\parallel}^{a_1} \sin^2\theta_V + I_{1c,\parallel(\perp)}^{a_1} \cos^2\theta_V \right. \\
&+ \left(I_{2s,\parallel(\perp)}^{a_1} \sin^2\theta_V + I_{2c,\parallel(\perp)}^{a_1} \cos^2\theta_V \right) \cos 2\theta_l \\
&+ \left(I_{6s,\parallel(\perp)}^{a_1} \sin^2\theta_V + I_{6c,\parallel(\perp)}^{a_1} \cos^2\theta_V \right) \cos\theta_l \\
&+ \left(I_{3,\parallel(\perp)}^{a_1} \cos 2\phi + I_{9,\parallel(\perp)}^{a_1} \sin 2\phi \right) \sin^2\theta_V \sin^2\theta_l \\
&+ \left(I_{4,\parallel(\perp)}^{a_1} \cos\phi + I_{8,\parallel(\perp)}^{a_1} \sin\phi \right) \sin 2\theta_V \sin 2\theta_l \\
&+ \left. \left(I_{5,\parallel(\perp)}^{a_1} \cos\phi + I_{7,\parallel(\perp)}^{a_1} \sin\phi \right) \sin 2\theta_V \sin\theta_l \right]. \tag{48}
\end{aligned}$$

where, $I_{n\lambda,\parallel}^{a_1}$ and $I_{n\lambda,\perp}^{a_1}$ are the angular coefficients. The explicit expressions of $I_{n\lambda,\parallel}^{a_1}$ in terms of the helicity amplitudes are written as,

$$\begin{aligned}
I_{1s,\parallel}^{a_1} &= \frac{(2 + \beta_l^2)}{2} N^2 (|H_+^1|^2 + |H_+^2|^2 + |H_-^1|^2 + |H_-^2|^2) \\
&+ \frac{4m_l^2}{q^2} N^2 (|H_+^1|^2 - |H_+^2|^2 + |H_-^1|^2 - |H_-^2|^2), \tag{49}
\end{aligned}$$

$$I_{1c,\parallel}^{a_1} = 2N^2 (|H_0^1|^2 + |H_0^2|^2) + \frac{8m_l^2}{q^2} N^2 (|H_0^1|^2 - |H_0^2|^2 + 2|H_t^2|^2), \tag{50}$$

$$I_{2s,\parallel}^{a_1} = \frac{\beta_l^2}{2} N^2 (|H_+^1|^2 + |H_+^2|^2 + |H_-^1|^2 + |H_-^2|^2), \tag{51}$$

$$I_{2c,\parallel}^{a_1} = -2\beta_l^2 N^2 (|H_0^1|^2 + |H_0^2|^2), \tag{52}$$

$$I_{3,\parallel}^{a_1} = -2\beta_l^2 N^2 \left[\mathcal{R}e (H_+^1 H_-^{1*} + H_+^2 H_-^{2*}) \right], \tag{53}$$

$$I_{4,\parallel}^{a_1} = \beta_l^2 N^2 \left[\mathcal{R}e (H_+^1 H_0^{1*} + H_-^1 H_0^{1*}) + \mathcal{R}e (H_+^2 H_0^{2*} + H_-^2 H_0^{2*}) \right], \tag{54}$$

$$I_{5,\parallel}^{a_1} = -2\beta_l N^2 \left[\mathcal{R}e (H_+^1 H_0^{2*} - H_-^1 H_0^{2*}) + \mathcal{R}e (H_+^2 H_0^{1*} - H_-^2 H_0^{1*}) \right], \tag{55}$$

$$I_{6s,\parallel}^{a_1} = -4\beta_l N^2 \left[\mathcal{R}e (H_+^1 H_+^{2*} - H_-^1 H_-^{2*}) \right], \tag{56}$$

$$I_{6c,\parallel}^{a_1} = 0, \tag{57}$$

$$I_{7,\parallel}^{a_1} = -2\beta_l N^2 \left[\mathcal{I}m (H_0^1 H_+^{2*} + H_0^1 H_-^{2*}) + \mathcal{I}m (H_0^2 H_+^{1*} + H_0^2 H_-^{1*}) \right], \tag{58}$$

$$I_{8,\parallel}^{a_1} = \beta_l^2 N^2 \left[\mathcal{I}m (H_0^1 H_+^{1*} - H_0^1 H_-^{1*}) + \mathcal{I}m (H_0^2 H_+^{2*} - H_0^2 H_-^{2*}) \right], \tag{59}$$

$$I_{9,\parallel}^{a_1} = 2\beta_l^2 N^2 \left[\mathcal{I}m (H_+^1 H_-^{1*} + H_+^2 H_-^{2*}) \right], \tag{60}$$

whereas the expressions of $I_{n\lambda,\perp}^{a_1}$ in terms of the helicity amplitudes are written as,

$$I_{1s,\perp}^{a_1} = \frac{(2 + \beta_l^2)}{4} N^2 (|H_+^1|^2 + |H_+^2|^2 + |H_-^1|^2 + |H_-^2|^2) + (|H_0^1|^2 + |H_0^2|^2) + \frac{2m_l^2}{q^2} N^2 \left[(|H_+^1|^2 - |H_+^2|^2 + |H_-^1|^2 - |H_-^2|^2) + 2(|H_0^1|^2 - |H_0^2|^2 + 2|H_t^2|^2) \right], \quad (61)$$

$$I_{1c,\perp}^{a_1} = \frac{(2 + \beta_l^2)}{2} N^2 (|H_+^1|^2 + |H_+^2|^2 + |H_-^1|^2 + |H_-^2|^2) + \frac{4m_l^2}{q^2} N^2 (|H_+^1|^2 - |H_+^2|^2 + |H_-^1|^2 - |H_-^2|^2), \quad (62)$$

$$I_{2s,\perp}^{a_1} = -\beta_l^2 N^2 \left[(|H_0^1|^2 + |H_0^2|^2) - \frac{1}{4} (|H_+^1|^2 + |H_+^2|^2 + |H_-^1|^2 + |H_-^2|^2) \right], \quad (63)$$

$$I_{2c,\perp}^{a_1} = \frac{\beta_l^2}{2} N^2 (|H_+^1|^2 + |H_+^2|^2 + |H_-^1|^2 + |H_-^2|^2), \quad (64)$$

$$I_{3,\perp}^{a_1} = \beta_l^2 N^2 \left[\mathcal{R}e (H_+^1 H_-^{1*} + H_+^2 H_-^{2*}) \right], \quad (65)$$

$$I_{4,\perp}^{a_1} = -\frac{\beta_l^2}{2} N^2 \left[\mathcal{R}e (H_+^1 H_0^{1*} + H_-^1 H_0^{1*}) + \mathcal{R}e (H_+^2 H_0^{2*} + H_-^2 H_0^{2*}) \right], \quad (66)$$

$$I_{5,\perp}^{a_1} = \beta_l N^2 \left[\mathcal{R}e (H_+^1 H_0^{2*} - H_-^1 H_0^{2*}) + \mathcal{R}e (H_+^2 H_0^{1*} - H_-^2 H_0^{1*}) \right], \quad (67)$$

$$I_{6s,\perp}^{a_1} = -2\beta_l N^2 \left[\mathcal{R}e (H_+^1 H_+^{2*} - H_-^1 H_-^{2*}) \right], \quad (68)$$

$$I_{6c,\perp}^{a_1} = -4\beta_l N^2 \left[\mathcal{R}e (H_+^1 H_+^{2*} - H_-^1 H_-^{2*}) \right], \quad (69)$$

$$I_{7,\perp}^{a_1} = \beta_l N^2 \left[\mathcal{I}m (H_0^1 H_+^{2*} + H_0^1 H_-^{2*}) + \mathcal{I}m (H_0^2 H_+^{1*} + H_0^2 H_-^{1*}) \right], \quad (70)$$

$$I_{8,\perp}^{a_1} = -\frac{\beta_l^2}{2} N^2 \left[\mathcal{I}m (H_0^1 H_+^{1*} - H_0^1 H_-^{1*}) + \mathcal{I}m (H_0^2 H_+^{2*} - H_0^2 H_-^{2*}) \right], \quad (71)$$

$$I_{9,\perp}^{a_1} = -\beta_l^2 N^2 \left[\mathcal{I}m (H_+^1 H_-^{1*} + H_+^2 H_-^{2*}) \right], \quad (72)$$

where

$$N = V_{tb} V_{td}^* \left[\frac{G_F^2 \alpha^2}{3.2^{10} \pi^5 m_B^3} q^2 \sqrt{\lambda} \beta_l \right]^{1/2}, \quad (73)$$

with $\lambda \equiv \lambda(m_B^2, m_M^2, q^2)$ and $\beta_l = \sqrt{1 - 4m_l^2/q^2}$.

2.7 Physical Observables for $B \rightarrow \rho(\rightarrow \pi\pi)\mu^+\mu^-$ Decay

In this section, we give the expressions of the physical observables such as the differential decay rate, lepton forward-backward asymmetry, longitudinal helicity fraction of ρ and the normalized angular observables $\langle I_{n\lambda}^\rho \rangle$, for $B \rightarrow \rho(\rightarrow \pi\pi)\mu^+\mu^-$ decay.

(i) Differential decay rate: From the full angular distribution Eq. (35), integration over

$\cos \theta_l = [-1, 1]$, $\cos \theta_V = [-1, 1]$, and $\phi = [0, 2\pi]$ yields the q^2 dependent differential decay rate expression, which in terms of the angular coefficients is as follows,

$$\frac{d\Gamma(B \rightarrow \rho(\rightarrow \pi\pi)\mu^+\mu^-)}{dq^2} = \mathcal{B}(\rho \rightarrow \pi\pi) \frac{1}{4} (3I_{1c}^\rho + 6I_{1s}^\rho - I_{2c}^\rho - 2I_{2s}^\rho). \quad (74)$$

(ii) Lepton forward-backward asymmetry: From the full angular distribution Eq. (35), the integration over $\cos \theta_V = [-1, 1]$, and $\phi = [0, 2\pi]$, gives the double differential decay rate $\left(\frac{d^2\Gamma}{dq^2 d\cos\theta_\ell}\right)$. The lepton forward-backward asymmetry corresponding to θ_ℓ is $A_{\text{FB}} = (F - B)/(F + B)$, where F and B are the forward and backward hemispheres. The forward backward asymmetry for $B \rightarrow \rho\mu^+\mu^-$ decay can be obtained by integrating $\frac{d^2\Gamma}{dq^2 d\cos\theta_\ell}$, and is defined as,

$$A_{\text{FB}}^\rho(q^2) = \frac{\int_0^1 \frac{d^2\Gamma}{dq^2 d\cos\theta_\ell} d\cos\theta_\ell - \int_{-1}^0 \frac{d^2\Gamma}{dq^2 d\cos\theta_\ell} d\cos\theta_\ell}{\int_{-1}^1 \frac{d^2\Gamma}{dq^2 d\cos\theta_\ell} d\cos\theta_\ell}. \quad (75)$$

In terms of the angular coefficients I 's the lepton forward-backward asymmetry for $B \rightarrow \rho(\rightarrow \pi\pi)\mu^+\mu^-$ as a function of q^2 can be expressed as,

$$A_{\text{FB}}^\rho(q^2) = \frac{6I_{6s}^\rho}{2(3I_{1c}^\rho + 6I_{1s}^\rho - I_{2c}^\rho - 2I_{2s}^\rho)}. \quad (76)$$

(iii) Longitudinal helicity fraction: From the full angular distribution Eq. (35), the integration over $\cos \theta_l = [-1, 1]$, and $\phi = [0, 2\pi]$, gives the double differential decay rate $\left(\frac{d^2\Gamma}{dq^2 d\cos\theta_V}\right)$. The longitudinal helicity fraction of the decay $B \rightarrow \rho(\rightarrow \pi\pi)\mu^+\mu^-$, when ρ meson is longitudinally polarized can be defined as,

$$f_L^\rho(q^2) = \frac{\int_{-1}^1 \frac{d^2\Gamma}{dq^2 d\cos\theta_V} \left(\frac{5}{2} \cos^2 \theta_V - \frac{1}{2}\right) d\cos\theta_V}{d\Gamma(B \rightarrow \rho(\rightarrow \pi\pi)\mu^+\mu^-)/dq^2}. \quad (77)$$

In terms of the angular coefficients I 's(q^2) the longitudinal helicity fraction for the decay $B \rightarrow \rho(\rightarrow \pi\pi)\mu^+\mu^-$ can be written as,

$$f_L^\rho(q^2) = \frac{3I_{1c}^\rho - I_{2c}^\rho}{3I_{1c}^\rho + 6I_{1s}^\rho - I_{2c}^\rho - 2I_{2s}^\rho}. \quad (78)$$

(iv) Normalized angular observables:

$$\langle I_{n\lambda}^\rho \rangle = \frac{\mathcal{B}(\rho \rightarrow \pi\pi) I_{n\lambda}^\rho}{d\Gamma(B \rightarrow \rho(\rightarrow \pi\pi)\mu^+\mu^-)/dq^2}. \quad (79)$$

(v) Binned normalized angular observables:

$$\langle I_{n\lambda}^\rho \rangle_{[q_{\min}^2, q_{\max}^2]} = \frac{\int_{q_{\min}^2}^{q_{\max}^2} \mathcal{B}(\rho \rightarrow \pi\pi) I_{n\lambda}^\rho dq^2}{\int_{q_{\min}^2}^{q_{\max}^2} (d\Gamma(B \rightarrow \rho(\rightarrow \pi\pi)\mu^+\mu^-)/dq^2) dq^2}. \quad (80)$$

2.8 Physical Observables for $B \rightarrow a_1(\rightarrow \rho_{||,\perp}\pi)\mu^+\mu^-$ Decay

The formulas of physical observables for $B \rightarrow a_1(\rightarrow \rho_{||,\perp}\pi)\mu^+\mu^-$ decay can be expressed as,

(i) Differential decay rates:

$$\frac{d\Gamma(B \rightarrow a_1(\rightarrow \rho_{||}\pi)\mu^+\mu^-)}{dq^2} = \mathcal{B}(a_1 \rightarrow \rho_{||}\pi) \frac{1}{4} (3I_{1c,||}^{a_1} + 6I_{1s,||}^{a_1} - I_{2c,||}^{a_1} - 2I_{2s,||}^{a_1}). \quad (81)$$

$$\frac{d\Gamma(B \rightarrow a_1(\rightarrow \rho_\perp \pi)\mu^+\mu^-)}{dq^2} = \mathcal{B}(a_1 \rightarrow \rho_\perp \pi) \frac{1}{4} (3I_{1c,\perp}^{a_1} + 6I_{1s,\perp}^{a_1} - I_{2c,\perp}^{a_1} - 2I_{2s,\perp}^{a_1}). \quad (82)$$

$$\frac{d\Gamma(B \rightarrow a_1(\rightarrow \rho \pi)\mu^+\mu^-)}{dq^2} = \frac{d\Gamma(B \rightarrow a_1(\rightarrow \rho_{\parallel} \pi)\mu^+\mu^-)}{dq^2} + \frac{d\Gamma(B \rightarrow a_1(\rightarrow \rho_\perp \pi)\mu^+\mu^-)}{dq^2}. \quad (83)$$

(ii) Lepton forward-backward asymmetry: From the full angular distribution Eq. (48), the integration over $\cos \theta_V = [-1, 1]$, and $\phi = [0, 2\pi]$, gives the double differential decay rate $\left(\frac{d^2\Gamma_{\parallel(\perp)}}{dq^2 d\cos\theta_\ell}\right)$, where $\Gamma_{\parallel(\perp)} \equiv \Gamma(B \rightarrow a_1(\rightarrow \rho_{\parallel(\perp)} \pi)\mu^+\mu^-)$. The lepton forward-backward asymmetry corresponding to θ_ℓ can be obtained from these polarized double differential decay rates as

$$A_{\text{FB}}^{a_1}(q^2) \equiv \left[\int_0^1 d\cos\theta_\ell \frac{d^2\Gamma_{\parallel(\perp)}}{dq^2 d\cos\theta_\ell} - \int_{-1}^0 d\cos\theta_\ell \frac{d^2\Gamma_{\parallel(\perp)}}{dq^2 d\cos\theta_\ell} \right] / \frac{d\Gamma_{\parallel(\perp)}}{dq^2}, \quad (84)$$

which in terms of the angular coefficient functions is given by,

$$A_{\text{FB}}^{a_1}(q^2) = \frac{3(I_{6c,\perp}^{a_1} + 2I_{6s,\perp}^{a_1})}{2(3I_{1c,\perp}^{a_1} + 6I_{1s,\perp}^{a_1} - I_{2c,\perp}^{a_1} - 2I_{2s,\perp}^{a_1})} = \frac{6I_{6s,\parallel}^{a_1}}{2(3I_{1c,\parallel}^{a_1} + 6I_{1s,\parallel}^{a_1} - I_{2c,\parallel}^{a_1} - 2I_{2s,\parallel}^{a_1})}. \quad (85)$$

(iii) Longitudinal helicity fraction: From the full angular distribution Eq. (48), the integration over $\cos \theta_l = [-1, 1]$, and $\phi = [0, 2\pi]$, gives the double differential decay rate $\left(\frac{d^2\Gamma_{\parallel(\perp)}}{dq^2 d\cos\theta_V}\right)$. The longitudinal helicity fraction of the decay $B \rightarrow a_1\mu^+\mu^-$, when a_1 meson is longitudinally polarized can be defined as,

$$f_L^{a_1}(q^2) = \frac{\int_{-1}^1 \frac{d^2\Gamma_{\parallel}}{dq^2 d\cos\theta_V} \left(\frac{5}{2} \cos^2 \theta_V - \frac{1}{2}\right) d\cos\theta_V}{d\Gamma(B \rightarrow a_1(\rightarrow \rho_{\parallel} \pi)\mu^+\mu^-)/dq^2} = \frac{\int_{-1}^1 \frac{d^2\Gamma_{\perp}}{dq^2 d\cos\theta_V} (2 - 5 \cos^2 \theta_V) d\cos\theta_V}{d\Gamma(B \rightarrow a_1(\rightarrow \rho_\perp \pi)\mu^+\mu^-)/dq^2}, \quad (86)$$

which in terms of the angular coefficient functions is given by,

$$f_L^{a_1}(q^2) = \frac{3I_{1c,\parallel}^{a_1} - I_{2c,\parallel}^{a_1}}{3I_{1c,\parallel}^{a_1} + 6I_{1s,\parallel}^{a_1} - I_{2c,\parallel}^{a_1} - 2I_{2s,\parallel}^{a_1}} = \frac{(6I_{1s,\perp}^{a_1} - 2I_{2s,\perp}^{a_1}) - (3I_{1c,\perp}^{a_1} - I_{2c,\perp}^{a_1})}{3I_{1c,\perp}^{a_1} + 6I_{1s,\perp}^{a_1} - I_{2c,\perp}^{a_1} - 2I_{2s,\perp}^{a_1}}. \quad (87)$$

(iv) Normalized angular observables: We introduce the normalized angular observables

$$\langle \widehat{I}_{n\lambda,\parallel(\perp)}^{a_1} \rangle = \frac{\mathcal{B}(a_1 \rightarrow \rho_{\parallel(\perp)} \pi) I_{n\lambda,\parallel(\perp)}^{a_1}}{d\Gamma(B \rightarrow a_1(\rightarrow \rho \pi)\mu^+\mu^-)/dq^2}. \quad (88)$$

(v) Binned normalized angular observables:

$$\langle \widehat{I}_{n\lambda,\parallel(\perp)}^{a_1} \rangle_{[q_{\min}^2, q_{\max}^2]} = \frac{\int_{q_{\min}^2}^{q_{\max}^2} \mathcal{B}(a_1 \rightarrow \rho_{\parallel(\perp)} \pi) I_{n\lambda,\parallel(\perp)}^{a_1} dq^2}{\int_{q_{\min}^2}^{q_{\max}^2} (d\Gamma(B \rightarrow a_1(\rightarrow \rho \pi)\mu^+\mu^-)/dq^2) dq^2}. \quad (89)$$

To compute the branching ratios $\mathcal{B}(a_1 \rightarrow \rho_{\parallel(\perp)} \pi)$ given in Eq. (89), one needs the amplitude of the decay whose expression is given as follows [62]

$$\langle \rho(p_\rho, \eta) \pi(p_\pi) | a_1(k, \bar{\epsilon}) \rangle = g_1(\bar{\epsilon} \cdot \eta)(k \cdot p_\rho) + g_2(\bar{\epsilon} \cdot p_\rho)(k \cdot \eta), \quad (90)$$

where g_1, g_2 are strong coupling constants and $\bar{\epsilon}, \eta$ are the polarization of a_1 and ρ meson.

The form of $\mathcal{B}(a_1 \rightarrow \rho_{\parallel(\perp)}\pi)$ for longitudinal and transverse ρ meson can be written as,

$$\mathcal{B}(a_1 \rightarrow \rho_{\parallel(\perp)}\pi) = \frac{1}{\Gamma_{a_1}} \frac{|\vec{p}_\rho|}{24\pi m_{a_1}^2} \Gamma_{\parallel(\perp)}, \quad (91)$$

where $|\vec{p}_\rho| = \frac{1}{2m_{a_1}} \sqrt{\lambda(m_{a_1}^2, m_\rho^2, m_\pi^2)}$, and

$$\Gamma_{\parallel} = \frac{m_{a_1}^2}{m_\rho^2} [(m_\rho^2 + |\vec{p}_\rho|^2)g_1 + |\vec{p}_\rho|^2 g_2]^2, \quad (92)$$

$$\Gamma_{\perp} = 2g_1^2 m_{a_1}^2 |\vec{p}_\rho|^2 \left(1 + \frac{m_\rho^2}{|\vec{p}_\rho|^2}\right). \quad (93)$$

The coupling constants g_1 and g_2 can be related through the amplitude given in [63]

$$\langle \rho(p_\rho, \eta)\pi(p_\pi) | a_1(k, \bar{\epsilon}) \rangle = -\frac{2\lambda_{a_1\rho\pi}}{m_\rho m_{a_1}} [(k \cdot p_\rho)(\bar{\epsilon} \cdot \eta) - (\bar{\epsilon} \cdot p_\rho)(k \cdot \eta)] \quad (94)$$

Comparing Eq. (90), and (94) gives $g_1 = -g_2 = \frac{2\lambda_{a_1\rho\pi}}{m_\rho m_{a_1}}$. Using the numerical values of masses from [64], one gets $\mathcal{B}(a_1 \rightarrow \rho_{\parallel}\pi) = 17.2\%$, and $\mathcal{B}(a_1 \rightarrow \rho_{\perp}\pi) = 43\%$. These values of branching ratios are used to analyze the above mentioned physical observables.

3 Numerical Analysis

3.1 Input Parameters

To analyze the signatures of family non-universal Z' gauge boson in the observables that belongs to $B \rightarrow (\rho, a_1)\mu^+\mu^-$ decays, we use the input parameters such as hadronic transition form factors, which are calculated in the framework of Light cone sum rules (LCSR) for the case of $B \rightarrow \rho(\pi\pi)\mu^+\mu^-$ decay [46], and in perturbative QCD (pQCD) approach for the case of $B \rightarrow a_1(\rightarrow \rho\pi)\mu^+\mu^-$ decay [47].

Table 1: Masses of resonances of quantum numbers J^P as represented for the parametrization of the form factors F_i for $b \rightarrow d$ transition.

F_i	J^P	$m_{R,i}^{b \rightarrow d}$
A_0	0^-	5.279
T_1, V	1^-	5.325
T_2, T_{23}, A_1, A_{12}	1^+	5.274

The combined fit of the simplified series expansion (SSE) parametrization to LCSR results for $B \rightarrow \rho(\pi\pi)\mu^+\mu^-$ are given as follows [46]

$$z(t) = \frac{\sqrt{t_+ - t} - \sqrt{t_+ - t_0}}{\sqrt{t_+ - t} + \sqrt{t_+ - t_0}}, \quad (95)$$

where, $t_{\pm} \equiv (m_B \pm m_\rho)^2$ and $t_0 \equiv t_+ \left(1 - \sqrt{1 - \frac{t_-}{t_+}}\right)$. We can write the expressions of the transition form factors for the decay $B \rightarrow \rho$ as,

$$F_i(q^2) = P_i(q^2) \sum_k \alpha_k^i [z(q^2) - z(0)]^k, \quad (96)$$

where $P_i(q^2) = \frac{1}{(1 - \frac{q^2}{m_{R,i}^2})}$, is a simple pole corresponding to the first resonance in the spectrum.

The resonance masses and the fit results for the SSE expansion coefficients in the fit to the LCSR computation for the decay $B \rightarrow \rho$ are presented in Table 1 and Table 2.

Table 2: Fit results for the SSE expansion coefficients in the fit to the LCSR computation for the decay $B \rightarrow \rho$ [46] decay.

	A_0	A_1	A_{12}	V	T_1	T_2	T_{23}
α_0	0.36 ± 0.04	0.26 ± 0.03	0.30 ± 0.03	0.33 ± 0.03	0.27 ± 0.03	0.27 ± 0.03	0.75 ± 0.08
α_1	-0.83 ± 0.20	0.39 ± 0.14	0.76 ± 0.20	-0.86 ± 0.18	-0.74 ± 0.14	0.47 ± 0.13	1.90 ± 0.43
α_2	1.33 ± 1.05	0.16 ± 0.41	0.46 ± 0.76	1.80 ± 0.97	1.45 ± 0.77	0.58 ± 0.46	2.93 ± 1.81

For $B \rightarrow a_1$ decay, the transition form factors were calculated in the framework of pQCD approach. The form factors that are involved in $B \rightarrow a_1$ decay, can be parametrized in the whole kinematical q^2 region as follows [47],

$$F(q^2) = \frac{F(0)}{1 - a(q^2/m_B^2) + b(q^2/m_B^2)^2}. \quad (97)$$

The numerical results for $B \rightarrow a_1$ decay at $q^2 = 0$, in the pQCD approach are presented in Table 3. The numerical values of Wilson coefficients in the SM, evaluated at the renormalization scale

Table 3: The numerical values of transition form factors for $B \rightarrow a_1$ decay at $q^2 = 0$, and the fitted parameters a and b [47].

	A	V_0	V_1	V_2	T_1	T_2	T_3
$F(0)$	$0.26^{+0.09}_{-0.09}$	$0.34^{+0.16}_{-0.17}$	$0.43^{+0.15}_{-0.15}$	$0.13^{+0.03}_{-0.04}$	$0.34^{+0.13}_{-0.13}$	$0.34^{+0.13}_{-0.13}$	$0.37^{+0.17}_{-0.12}$
a	$1.72^{+0.05}_{-0.05}$	$1.73^{+0.05}_{-0.06}$	$0.75^{+0.05}_{-0.05}$	--	$1.60^{+0.06}_{-0.05}$	$0.71^{+0.07}_{-0.05}$	$1.60^{+0.06}_{-0.05}$
b	$0.66^{+0.07}_{-0.06}$	$0.66^{+0.06}_{-0.08}$	$-0.12^{+0.05}_{-0.02}$	--	$0.53^{+0.06}_{-0.04}$	$-0.16^{+0.03}_{-0.02}$	$0.53^{+0.06}_{-0.04}$

$\mu \sim m_b$ [65], are presented in Table 4. In order to analyze the normalized angular observables

Table 4: The numerical values of the SM Wilson coefficients up to NNLL accuracy, evaluated at the renormalization scale $\mu \sim m_b$ [65].

C_1	C_2	C_3	C_4	C_5	C_6	C_7	C_8	C_9	C_{10}
-0.294	1.017	-0.0059	-0.087	0.0004	0.0011	-0.324	-0.176	4.114	-4.193

and the other observables such as differential branching ratios, forward-backward asymmetry, longitudinally polarized final state vector and axial vector mesons in $B \rightarrow \rho(\rightarrow \pi\pi)\mu^+\mu^-$ and $B \rightarrow a_1(\rightarrow \rho_{\perp,\parallel})\mu^+\mu^-$ decays, respectively, in the framework of the family non-universal Z' model, the numerical values of Z' model parameters are collected in Table 5.

To gauge the effects of family non-universal Z' model in the above mentioned physical observables, the numerical values of coupling B_{db}^L and the weak phase ϕ_{db} presented in Table 5 are fixed, and are constrained from $B_q^0 - \bar{B}_q^0$ mixing [66]. The scenarios S1(S2) given in Table 5

Table 5: The numerical values of lepton and quark coupling in Z' model are collected from Ref. [43].

Scenarios	$ B_{db}^L \times 10^{-3}$	ϕ_{db} in degrees	S_{LR}	D_{LR}
S1	0.16 ± 0.08	-33 ± 45	0.08	-0.02
S2	0.12 ± 0.03	-23 ± 21	0.08	-0.02

represents the constraints from UTfit collaboration on the parameters C_{B_q} and ϕ_{B_q} [67]. The explicit form of C_{B_q} and ϕ_{B_q} is given by,

$$C_{B_q} e^{2i\phi_{B_q}} \equiv \frac{\langle B_q | H_{\text{eff}}^{\text{full}} | \bar{B}_q \rangle}{\langle B_q | H_{\text{eff}}^{\text{SM}} | \bar{B}_q \rangle} \quad (98)$$

Using the maximum allowed values of the coupling constants given in Table 5, the numerical values of the non-universal family Z' model Wilson coefficients $C_9^{Z'}$ and $C_{10}^{Z'}$ in scenarios S1 and S2 are presented in Table 6.

Table 6: The numerical values of family non-universal Z' model Wilson coefficients $C_9^{Z'}$ and $C_{10}^{Z'}$ in scenarios S1 and S2.

	S1	S2
$C_9^{Z'}$	0.0000192	0.000012
$C_{10}^{Z'}$	-4.8×10^{-6}	-3.0×10^{-6}

3.2 Phenomenological Analysis of the Physical Observables in $B \rightarrow \rho(\rightarrow \pi\pi)\mu^+\mu^-$ and $B \rightarrow a_1(\rightarrow \rho_{\parallel,\perp}\pi)\mu^+\mu^-$ Decays

In this section, we present our phenomenological analysis of the family non-universal Z' model via physical observables constructed from the combination of different angular coefficients such as the differential branching ratios ($d\mathcal{B}/dq^2$), lepton forward-backward asymmetry (A_{FB}), longitudinal polarization fraction (f_L) of ρ and a_1 mesons, in the $B \rightarrow \rho(\rightarrow \pi\pi)\mu^+\mu^-$ and $B \rightarrow a_1(\rightarrow \rho_{\parallel,\perp})\mu^+\mu^-$ decays, respectively. The predicted numerical values of these observables, in different q^2 bins, for the SM as well as for the two different scenarios of family non-universal Z' model are given in Tables 7-14, of appendix B. The listed errors in these tables originate mainly from the uncertainties of the form factors. Furthermore, in Figs. 2-3, we have plotted the above mentioned physical observables as a function of q^2 . Following are our predictions regarding the physical observables.

- Figs. 2(a), 2(b), 2(c), and 2(d) depict the differential branching ratios $\frac{d\mathcal{B}}{dq^2}$ of $B \rightarrow \rho(\rightarrow \pi\pi)\mu^+\mu^-$, $B \rightarrow a_1(\rightarrow \rho\pi)\mu^+\mu^-$, $B \rightarrow a_1(\rightarrow \rho_{\parallel}\pi)\mu^+\mu^-$ and $B \rightarrow a_1(\rightarrow \rho_{\perp}\pi)\mu^+\mu^-$ decays, respectively, in the framework of the SM and the scenarios S1 and S2 of the family non-universal Z' model. Fig. 2(a) indicates that, after including uncertainties of the form factors, the predictions of differential branching ratio in two scenarios of the family non-universal Z' model deviate from the SM predictions such that they show a tendency towards higher values of differential branching ratios as compared to the SM expectations, which is more dominant in Scenario S1. In Figs. 2(b), 2(c), and 2(d), our results show similar trend of higher values of differential branching ratios in two scenarios of the family non-universal Z' model, however in this case SM predictions largely overlap

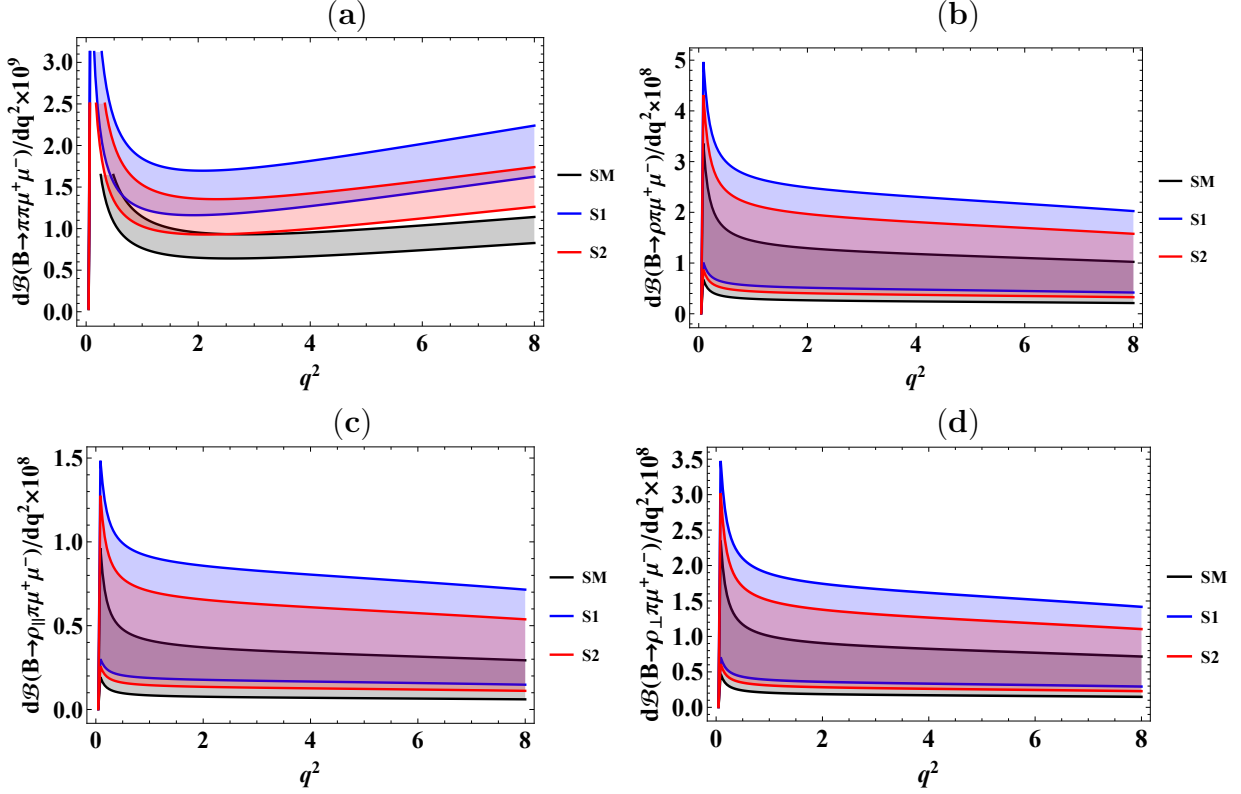


Figure 2: Differential branching ratio of the decay (a) $B \rightarrow \rho(\rightarrow \pi\pi)\mu^+\mu^-$, (b) $B \rightarrow a_1(\rightarrow \rho\pi)\mu^+\mu^-$, (c) $B \rightarrow a_1(\rightarrow \rho_{\parallel}\pi)\mu^+\mu^-$, and (d) $B \rightarrow a_1(\rightarrow \rho_{\perp}\pi)\mu^+\mu^-$, in the SM and the two scenarios of the family non-universal Z' model.

with the scenarios of the family non-universal Z' model due to the larger uncertainties originating from the form factors. At very low $q^2 < 1 \text{ GeV}^2$, these differential branching ratios are dominated by the SM magnetic dipole Wilson coefficient C_7 , so at $q^2 \rightarrow 0$, the results of differential branching ratios indicate singularity corresponding to photon pole.

- Figs. 3 represents the lepton forward-backward asymmetry and longitudinally polarized final state mesons as a function of q^2 in the framework of the SM and the family non-universal Z' model for $B \rightarrow \rho\mu^+\mu^-$ and $B \rightarrow a_1\mu^+\mu^-$ decays. Figs. 3(a) and fig. 3(c) show the zero position of the $A_{\text{FB}}(q^2)$ for $B \rightarrow \rho\mu^+\mu^-$ and $B \rightarrow a_1\mu^+\mu^-$ decays in the framework of SM and two scenarios S1 and S2 of family non-universal Z' model, respectively. Both scenarios S1 and S2 of the family non-universal Z' are shifted towards left as compared to the SM prediction, as a result, the zero crossing of $A_{\text{FB}}^{\rho}(q^2)$ and $A_{\text{FB}}^{a_1}(q^2)$ for both scenarios is distinguishable from the SM expectation. Also overall q^2 predictions of $A_{\text{FB}}^{\rho}(q^2)$ and $A_{\text{FB}}^{a_1}(q^2)$ in the S1 and S2 scenarios for the whole q^2 range show discrimination from the SM results. In Fig. 3(b), we have plotted the longitudinal helicity fraction f_L^{ρ} , for the decay $B \rightarrow \rho\mu^+\mu^-$ decay in the SM framework and the two scenarios S1, S2 of the family non universal Z' model. The predictions in S1 and S2 scenarios, clearly show a departure from the SM result in the region $q^2 = (0.1 - 5) \text{ GeV}^2$. However, for the case of $B \rightarrow a_1\mu^+\mu^-$ decay, longitudinal helicity fraction $f_L^{a_1}$, shows deviation from the SM result in the region $q^2 = (0.1 - 3) \text{ GeV}^2$, only as shown in fig. 3(d). From the values of the NP Wilson coefficients reported in Table 6, it is evident that the SM Wilson coefficients get more pronounced deviations in the presence of scenario

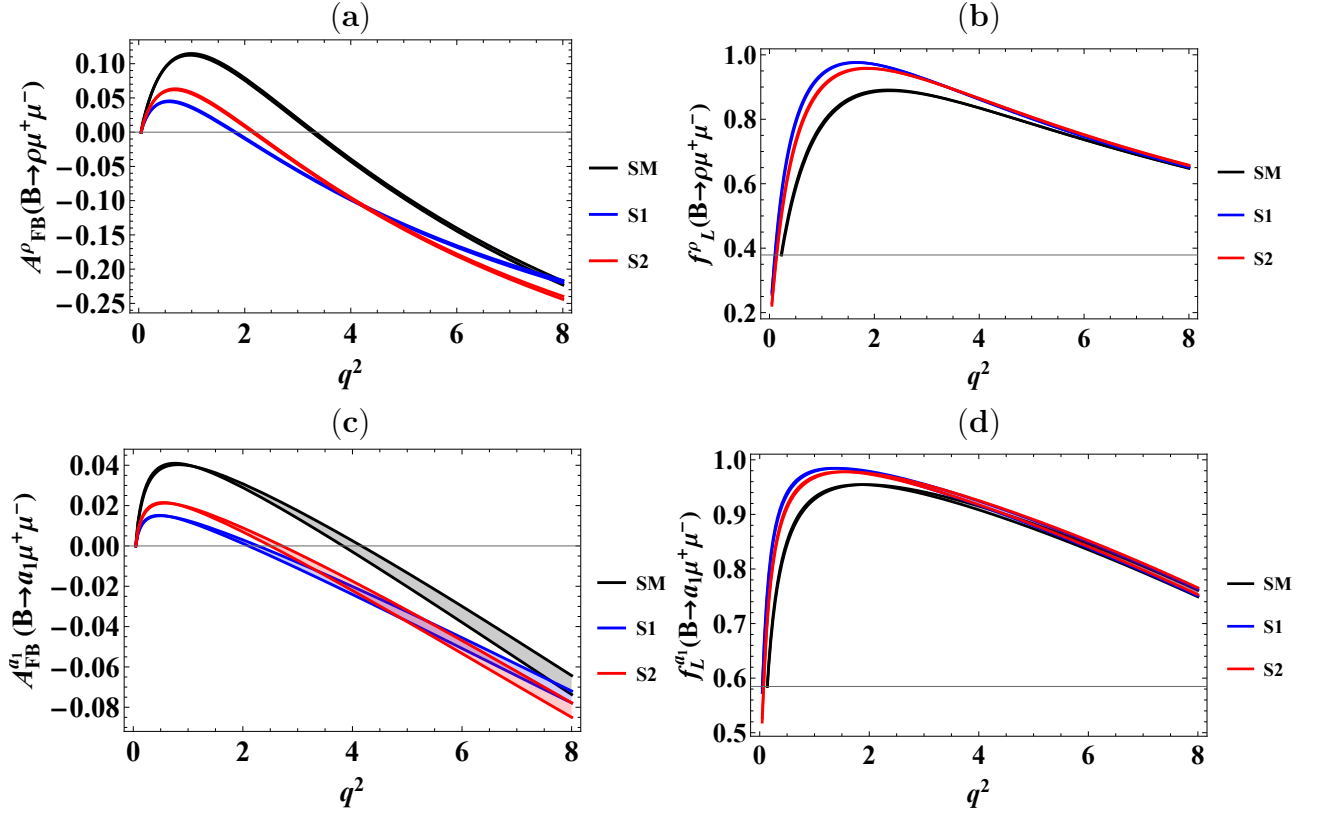


Figure 3: (a) Lepton forward-backward asymmetry A_{FB}^ρ , (b) longitudinal polarization fraction of ρ meson f_L^ρ , for the $B \rightarrow \rho\mu^+\mu^-$ decay, while (c) Lepton forward-backward asymmetry $A_{\text{FB}}^{a_1}$, (d) longitudinal polarization fraction of a_1 meson $f_L^{a_1}$, for the $B \rightarrow a_1\mu^+\mu^-$ decay in the SM and the two scenarios of the family non-universal Z' model.

S1, compared to scenario S2, which also reflects in the overall results of observables such that scenario S2 appears closer to the SM.

3.3 Phenomenological analysis of the Angular coefficients in $B \rightarrow \rho(\rightarrow \pi\pi)\mu^+\mu^-$ and $B \rightarrow a_1(\rightarrow \rho_{\parallel,\perp}\pi)\mu^+\mu^-$ Decays

In this section, we present the effects of the family non-universal Z' model on the separate normalized angular coefficients such as $\langle I_{n\lambda}^\rho \rangle$, in the $B \rightarrow \rho(\rightarrow \pi\pi)\mu^+\mu^-$ decay, and $\langle \hat{I}_{n\lambda,\parallel}^{a_1} \rangle$, $\langle \hat{I}_{n\lambda,\perp}^{a_1} \rangle$, in the $B \rightarrow a_1(\rightarrow \rho_{\parallel,\perp})\mu^+\mu^-$ decays. The predicted numerical values of these observables, in different q^2 bins, for the SM as well as for the two different scenarios of family non-universal Z' model are given in Tables 15-38, of appendix B. The listed errors in these tables originate mainly from the uncertainties of the form factors. Furthermore, we also display the results of normalized angular observables as a function of q^2 in Figs. 4-6.

- Fig. 4 depicts the normalized angular observables $\langle I_{1s}^\rho \rangle$, $\langle I_{2s}^\rho \rangle$, $\langle I_{1c}^\rho \rangle$, $\langle I_{2c}^\rho \rangle$, $\langle I_3^\rho \rangle$, $\langle I_4^\rho \rangle$, $\langle I_5^\rho \rangle$ and $\langle I_{6s}^\rho \rangle$ for $B \rightarrow \rho(\rightarrow \pi\pi)\mu^+\mu^-$ decay in the SM and the two scenarios S1, S2 of family non universal Z' model. Figs. 4(a)-4(d) show clear discrimination between the SM predictions and the two scenarios S1 and S2 of the family non-universal Z' model for the angular observables $\langle I_{1s}^\rho \rangle$, $\langle I_{2s}^\rho \rangle$, $\langle I_{1c}^\rho \rangle$ and $\langle I_{2c}^\rho \rangle$ in the range of $q^2 = (0.1 - 7)$ GeV². Furthermore, the angular observables $\langle I_3^\rho \rangle$, $\langle I_4^\rho \rangle$, $\langle I_5^\rho \rangle$ and $\langle I_{6s}^\rho \rangle$ are shown in Fig. 4(e)-4(h). For the observables $\langle I_3^\rho \rangle$ and $\langle I_4^\rho \rangle$ shown in Fig. 4(e) and 4(f), the SM predictions

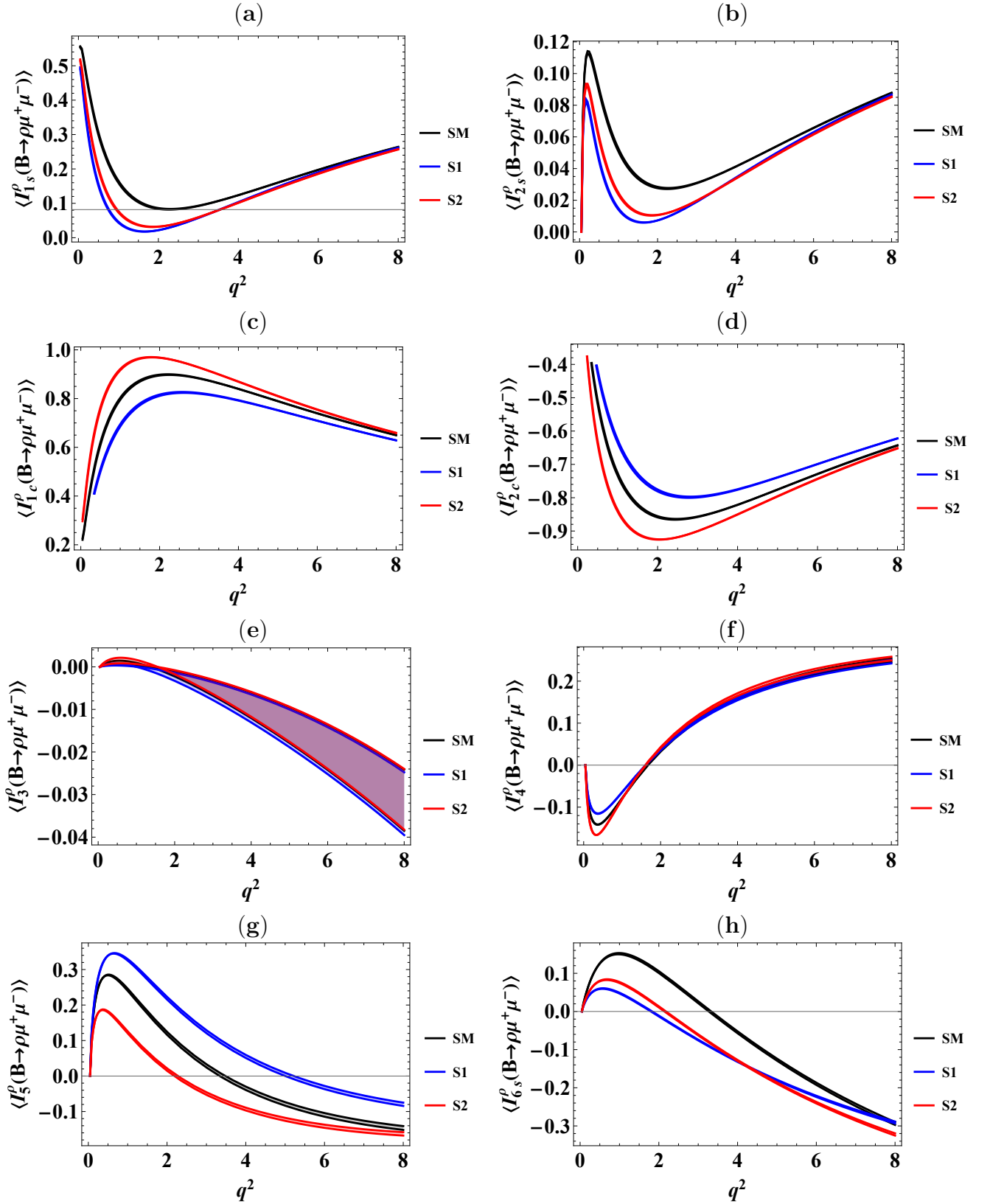


Figure 4: Angular observables $\langle I_{1s}^\rho \rangle, \langle I_{2s}^\rho \rangle, \langle I_{1c}^\rho \rangle, \langle I_{2c}^\rho \rangle, \langle I_3^\rho \rangle, \langle I_4^\rho \rangle, \langle I_5^\rho \rangle$, and $\langle I_{6s}^\rho \rangle$ for the decay $B \rightarrow \rho(\rightarrow \pi\pi)\mu^+\mu^-$, in the SM and the two scenarios of the family non-universal Z' model.

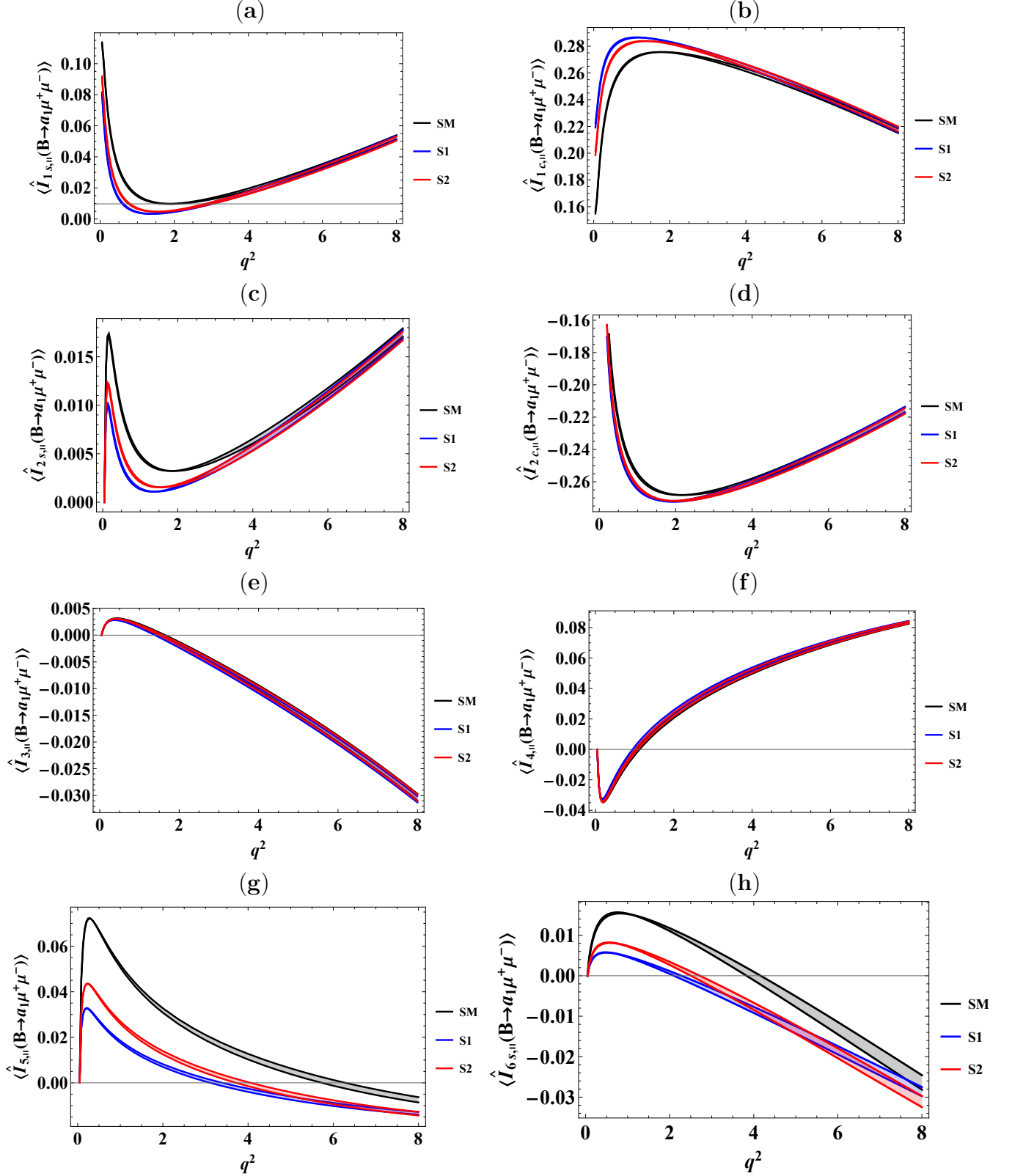


Figure 5: Angular observables $\langle \hat{I}_{1s,\parallel}^{a_1} \rangle$, $\langle \hat{I}_{1c,\parallel}^{a_1} \rangle$, $\langle \hat{I}_{2s,\parallel}^{a_1} \rangle$, $\langle \hat{I}_{2c,\parallel}^{a_1} \rangle$, $\langle \hat{I}_{3,\parallel}^{a_1} \rangle$, $\langle \hat{I}_{4,\parallel}^{a_1} \rangle$, $\langle \hat{I}_{5,\parallel}^{a_1} \rangle$, and $\langle \hat{I}_{6s,\parallel}^{a_1} \rangle$ for the decay $B \rightarrow a_1(\rightarrow \rho_{\parallel}\pi)\mu^+\mu^-$, in the SM and the two scenarios of the family non-universal Z' model.

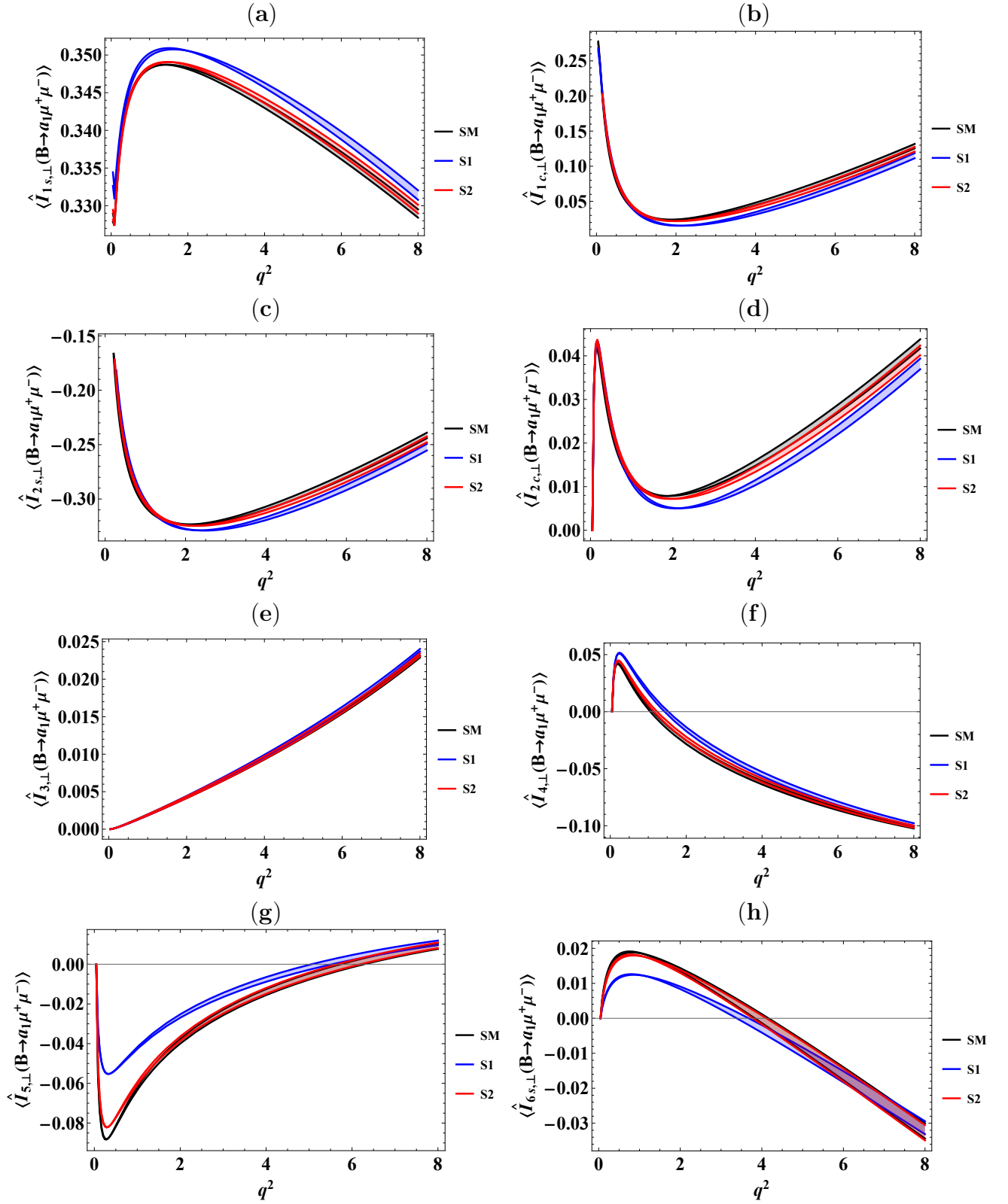


Figure 6: Angular observables $\langle \hat{I}_{1s,\perp}^{a_1} \rangle$, $\langle \hat{I}_{1c,\perp}^{a_1} \rangle$, $\langle \hat{I}_{2s,\perp}^{a_1} \rangle$, $\langle \hat{I}_{2c,\perp}^{a_1} \rangle$, $\langle \hat{I}_{3,\perp}^{a_1} \rangle$, $\langle \hat{I}_{4,\perp}^{a_1} \rangle$, $\langle \hat{I}_{5,\perp}^{a_1} \rangle$, and $\langle \hat{I}_{6s,\perp}^{a_1} \rangle$ for the decay $B \rightarrow a_1(\rightarrow \rho_\perp \pi) \mu^+ \mu^-$, in the SM and the two scenarios of the family non-universal Z' model.

and effects of the family non-universal Z' model overlap with each other and hence no discrimination can be observed for these observables, except for some region of q^2 near 0.5 GeV^2 for $\langle I_4^\rho \rangle$. For the observables $\langle I_5^\rho \rangle$ and $\langle I_{6s}^\rho \rangle$, the discrimination between the SM and two scenarios of the family non-universal Z' model can be found for almost the whole kinematical range of q^2 . Further, the two scenarios remain distinguishable from each other in almost the whole q^2 range.

- Fig. 5 presents the normalized angular observables $\langle \widehat{I}_{1s,\parallel}^{a_1} \rangle$, $\langle \widehat{I}_{1c,\parallel}^{a_1} \rangle$, $\langle \widehat{I}_{2s,\parallel}^{a_1} \rangle$, $\langle \widehat{I}_{2c,\parallel}^{a_1} \rangle$, $\langle \widehat{I}_{3,\parallel}^{a_1} \rangle$, $\langle \widehat{I}_{4,\parallel}^{a_1} \rangle$, $\langle \widehat{I}_{5,\parallel}^{a_1} \rangle$, and $\langle \widehat{I}_{6s,\parallel}^{a_1} \rangle$ for the $B \rightarrow a_1(\rightarrow \rho_{\parallel}\pi)\mu^+\mu^-$ decay in the SM as well as in S1 and S2 of the family non universal Z' model. Figs. 5(a)-5(d) show some discrimination between the SM predictions and the two scenarios S1 and S2 of the family non-universal Z' model for the angular observables $\langle \widehat{I}_{1s,\parallel}^{a_1} \rangle$, $\langle \widehat{I}_{1c,\parallel}^{a_1} \rangle$, $\langle \widehat{I}_{2s,\parallel}^{a_1} \rangle$, $\langle \widehat{I}_{2c,\parallel}^{a_1} \rangle$ in the range of $q^2 = (0.1 - 3) \text{ GeV}^2$, whereas the two scenarios are not much distinct from each other. Furthermore, the angular observables $\langle \widehat{I}_{3,\parallel}^{a_1} \rangle$, $\langle \widehat{I}_{4,\parallel}^{a_1} \rangle$, $\langle \widehat{I}_{5,\parallel}^{a_1} \rangle$, and $\langle \widehat{I}_{6s,\parallel}^{a_1} \rangle$ are shown in Fig. 5(e)-5(h). For the observables $\langle \widehat{I}_{3,\parallel}^{a_1} \rangle$ and $\langle \widehat{I}_{4,\parallel}^{a_1} \rangle$, no segregation is observed among SM and S1, S2 scenarios of the family non-universal Z' model as they are found to be largely overlapping with each other as shown in Fig. 5(e) and 5(f). For the observables $\langle \widehat{I}_{5,\parallel}^{a_1} \rangle$ and $\langle \widehat{I}_{6s,\parallel}^{a_1} \rangle$, the discrimination between the SM and two scenarios of the family non-universal Z' model can be found for almost the whole kinematical range of q^2 , whereas the two scenarios remain distinguishable from each other in the range of $q^2 = (0.1 - 4) \text{ GeV}^2$ and $q^2 = (0.1 - 2.5) \text{ GeV}^2$, for $\langle \widehat{I}_{5,\parallel}^{a_1} \rangle$ and $\langle \widehat{I}_{6s,\parallel}^{a_1} \rangle$, respectively, as shown in Fig. 5(g) and 5(h).
- Fig. 6 presents the normalized angular observables $\langle \widehat{I}_{1s,\perp}^{a_1} \rangle$, $\langle \widehat{I}_{1c,\perp}^{a_1} \rangle$, $\langle \widehat{I}_{2s,\perp}^{a_1} \rangle$, $\langle \widehat{I}_{2c,\perp}^{a_1} \rangle$, $\langle \widehat{I}_{3,\perp}^{a_1} \rangle$, $\langle \widehat{I}_{4,\perp}^{a_1} \rangle$, $\langle \widehat{I}_{5,\perp}^{a_1} \rangle$, and $\langle \widehat{I}_{6s,\perp}^{a_1} \rangle$ for the $B \rightarrow a_1(\rightarrow \rho_{\perp}\pi)\mu^+\mu^-$ decay in the SM as well as in S1 and S2 of the family non universal Z' model. Although the angular observable $\langle \widehat{I}_{6c,\perp}^{a_1} \rangle$ is non-zero, we do not present its results as its q^2 behaviour is similar to $\langle \widehat{I}_{6s,\perp}^{a_1} \rangle$, as coming from Eqs. (68), (69). In all the angular observables, scenario S1 of the family non-universal Z' model overlaps with the SM error band, whereas scenario S2 remains distinct from the SM and the scenario S1 in different ranges of the q^2 for different angular observables as shown in Fig. 6(a)-6(h).

4 Conclusions

Investigating B meson decays allows us to test the SM parameters along with exploring New Physics. Several exclusive semileptonic decays that involve flavor-changing neutral current transitions and flavor-changing charged current transitions exhibit notable deviations from SM predictions. Semileptonic decays involving $b \rightarrow s$ current have been studied during recent years and showed deviations from the SM predictions. In this work, the FCNC processes governed by $b \rightarrow d l^+ l^-$ transition have been studied in the family non-universal Z' model. The four-fold angular decay distributions of $B \rightarrow \rho(\rightarrow \pi\pi)\mu^+\mu^-$, and $B \rightarrow a_1(\rightarrow \rho_{\parallel,\perp}\pi)\mu^+\mu^-$ decays have been derived using the helicity formalism. For both decays, various physical observables have been extracted and studied in the SM and the two scenarios of the family non-universal Z' model.

To conclude the analysis, a noticeable difference has been observed between SM and the NP predicted values of the studied physical observables and in the majority of the normalized angular coefficients for the $B \rightarrow \rho(\rightarrow \pi\pi)\mu^+\mu^-$ decay, while the overall effect of NP is less distinct in most of the observables for the case of $B \rightarrow a_1(\rightarrow \rho_{\parallel,\perp}\pi)\mu^+\mu^-$ decay. For instance,

in case of the differential branching ratio the SM and the Z' model scenarios are distinguishable for $B \rightarrow \rho(\rightarrow \pi\pi)\mu^+\mu^-$ decay while no clear distinction has been observed for $B \rightarrow a_1\mu^+\mu^-$ decay. In case of the forward-backward asymmetry and the longitudinal polarization fraction, the pattern of deviations reported is similar for both decays, however, the distinction among the two scenarios appears for larger range of q^2 in case of $B \rightarrow \rho(\rightarrow \pi\pi)\mu^+\mu^-$ decay in comparison to $B \rightarrow a_1\mu^+\mu^-$ decay. Similarly, most of the normalized angular observables for the $B \rightarrow \rho(\rightarrow \pi\pi)\mu^+\mu^-$ decay show notable distinction between the SM and the scenarios (S1, S2) predictions of the family non-universal Z' model, whereas, except for some, most of the normalized angular observables for the $B \rightarrow a_1(\rightarrow \rho_{\parallel,\perp}\pi)\mu^+\mu^-$ decay, show little or no distinction between the SM and the NP scenarios in the family non-universal Z' model. Rare $b \rightarrow d\ell\ell$ decays can be studied at high luminosity flavor facilities, such as LHCb [68], and Belle II [69]. For the present study, measurements of various normalized angular observables of the order of 1% relative to the branching ratio of order 10^{-9} at 3σ level require approximately 10^{13} $B\bar{B}$ pairs, and for the integrated luminosity goal of 300 fb^{-1} in HL-LHC $\sim 10^{14}$ $b\bar{b}$ pairs are expected to be produced [68, 70]. Therefore, the precise measurements of these observables in experiments conducted at LHCb and future collider facilities appear to be possible and it will provide valuable supplementary data needed to elucidate the underlying characteristics of NP within $b \rightarrow d\ell^+\ell^-$ decays.

Acknowledgments

This work is supported by the Higher Education Commission of Pakistan through Grant no. NRPU/20-15142.

A Wilson Coefficients Expressions in the SM

The explicit expressions used for the Wilson coefficients are given as follows [39, 53–57],

$$\begin{aligned}
C_7^{\text{eff}}(q^2) &= C_7 - \frac{1}{3} \left(C_3 + \frac{4}{3}C_4 + 20C_5 + \frac{80}{3}C_6 \right) - \frac{\alpha_s}{4\pi} \left[(C_1 - 6C_2)F_{1,c}^{(7)}(q^2) + C_8F_8^{(7)}(q^2) \right] \\
&\quad - \frac{\alpha_s}{4\pi} \lambda_u^{(q)} (C_1 - 6C_2) (F_{1,c}^7 - F_{1,u}^7), \\
C_9^{\text{eff}}(q^2) &= C_9 + \frac{4}{3} \left(C_3 + \frac{16}{3}C_5 + \frac{16}{9}C_6 \right) - h(0, q^2) \left(\frac{1}{2}C_3 + \frac{2}{3}C_4 + 8C_5 + \frac{32}{3}C_6 \right) \\
&\quad - h(m_b^{\text{pole}}, q^2) \left(\frac{7}{2}C_3 + \frac{2}{3}C_4 + 38C_5 + \frac{32}{3}C_6 \right) + h(m_c^{\text{pole}}, q^2) \left(\frac{4}{3}C_1 + C_2 + 6C_3 + 60C_5 \right) \\
&\quad + \lambda_u^{(q)} [h(m_c, q^2) - h(0, q^2)] \left(\frac{4}{3}C_1 + C_2 \right) - \frac{\alpha_s}{4\pi} \left[C_1F_{1,c}^{(9)}(q^2) + C_2F_{2,c}^{(9)}(q^2) + C_8F_8^{(9)}(q^2) \right] \\
&\quad - \frac{\alpha_s}{4\pi} \lambda_u^{(q)} \left[C_1(F_{1,c}^{(9)} - F_{1,u}^{(9)}) + C_2(F_{2,c}^{(9)} - F_{2,u}^{(9)}) \right], \tag{99}
\end{aligned}$$

where the functions $h(m_q^{\text{pole}}, q^2)$ with $q = c, b$, and functions $F_8^{(7,9)}(q^2)$ are defined in [54], while the functions $F_{1,c}^{(7,9)}(q^2)$, $F_{2,c}^{(7,9)}(q^2)$ are given in [56] for low q^2 and in [57] for high q^2 . The quark masses appearing in all of these functions are defined in the pole scheme.

B Binned Predictions of Physical Observables

In this appendix, we give the SM as well as the family non-universal Z' model predictions of physical observables in different q^2 bins.

Table 7: Predictions of observables in the decay $B \rightarrow \rho(\rightarrow \pi\pi)\mu^+\mu^-$, such as differential branching ratios, $\frac{dB}{dq^2}(B \rightarrow \rho\mu^+\mu^-)$, $\frac{dB}{dq^2}(B \rightarrow \rho(\rightarrow \pi\pi)\mu^+\mu^-)$, lepton forward-backward asymmetry A_{FB}^ρ , longitudinal helicity fraction f_L^ρ , and in the decay $B \rightarrow a_1(\rightarrow \rho\pi)\mu^+\mu^-$, such as differential branching ratios $\frac{dB}{dq^2}(B \rightarrow a_1\mu^+\mu^-)$, $\frac{dB}{dq^2}(B \rightarrow a_1(\rightarrow \rho_{\parallel}\pi)\mu^+\mu^-)$, $\frac{dB}{dq^2}(B \rightarrow a_1(\rightarrow \rho_{\perp}\pi)\mu^+\mu^-)$, lepton forward-backward asymmetry $A_{\text{FB}}^{a_1}$, and longitudinal helicity fraction $f_L^{a_1}$, in $q^2 = 0.1-1.0$ GeV² bin, for the SM as well as the NP scenarios (S1, S2) of Z' model listed in Table 5. The errors presented mainly come from the uncertainties of the form factors.

$q^2 = 0.1 - 1.0 \text{ GeV}^2$			
Observables	SM	Z' Scenario 1	Z' Scenario 2
$\frac{dB}{dq^2}(B \rightarrow \rho\mu^+\mu^-) \times 10^{+9}$	$1.889_{-0.339}^{+0.339}$	$2.410_{-0.497}^{+0.497}$	$2.176_{-0.430}^{+0.430}$
$\frac{dB}{dq^2}(B \rightarrow \rho(\rightarrow \pi\pi)\mu^+\mu^-) \times 10^{+9}$	$1.889_{-0.339}^{+0.339}$	$2.410_{-0.497}^{+0.497}$	$2.176_{-0.430}^{+0.430}$
A_{FB}^ρ	$0.077_{-0.002}^{+0.002}$	$0.037_{-0.001}^{+0.001}$	$0.049_{-0.001}^{+0.001}$
f_L^ρ	$0.510_{-0.005}^{+0.005}$	$0.717_{-0.005}^{+0.005}$	$0.652_{-0.006}^{+0.006}$
$\frac{dB}{dq^2}(B \rightarrow a_1\mu^+\mu^-) \times 10^{+9}$	$11.1295_{-7.3804}^{+7.3804}$	$19.208_{-12.684}^{+12.684}$	$15.772_{-1.042}^{+1.042}$
$\frac{dB}{dq^2}(B \rightarrow a_1(\rightarrow \rho_{\parallel}\pi)\mu^+\mu^-) \times 10^{+9}$	$3.1905_{-2.1157}^{+2.1157}$	$5.506_{-3.636}^{+3.636}$	$4.521_{-2989}^{+2.989}$
$\frac{dB}{dq^2}(B \rightarrow a_1(\rightarrow \rho_{\perp}\pi)\mu^+\mu^-) \times 10^{+9}$	$7.7907_{-5.1663}^{+5.1663}$	$13.446_{-8.879}^{+8.879}$	$11.040_{-7.3001}^{+7.3001}$
$A_{\text{FB}}^{a_1}$	$0.0347_{-0.0005}^{+0.0005}$	$0.0135_{-0.00005}^{+0.00005}$	$0.0191_{-0.0002}^{+0.0002}$
$f_L^{a_1}$	$0.8022_{-0.0036}^{+0.0036}$	$0.7952_{-0.0034}^{+0.0034}$	$0.7910_{-0.0038}^{+0.0038}$

Table 8: Same as in Table 7, but for $q^2 = 1.0 - 2.0$ GeV² bin.

$q^2 = 1.0 - 2.0 \text{ GeV}^2$			
Observables	SM	Z' Scenario 1	Z' Scenario 2
$\frac{dB}{dq^2}(B \rightarrow \rho\mu^+\mu^-) \times 10^{+9}$	$0.856_{-0.166}^{+0.166}$	$1.462_{-0.279}^{+0.279}$	$1.188_{-0.275}^{+0.275}$
$\frac{dB}{dq^2}(B \rightarrow \rho(\rightarrow \pi\pi)\mu^+\mu^-) \times 10^{+9}$	$0.856_{-0.166}^{+0.166}$	$1.462_{-0.279}^{+0.279}$	$1.188_{-0.275}^{+0.275}$
A_{FB}^ρ	$0.100_{-0.002}^{+0.002}$	$0.015_{-0.001}^{+0.001}$	$0.035_{-0.001}^{+0.001}$
f_L^ρ	$0.840_{-0.001}^{+0.001}$	$0.968_{-0.001}^{+0.001}$	$0.943_{-0.001}^{+0.001}$
$\frac{dB}{dq^2}(B \rightarrow a_1\mu^+\mu^-) \times 10^{+9}$	$8.1566_{-5.3824}^{+5.3824}$	$15.5392_{-10.2335}^{+10.2335}$	$12.330_{-8.125}^{+8.125}$
$\frac{dB}{dq^2}(B \rightarrow a_1(\rightarrow \rho_{\parallel}\pi)\mu^+\mu^-) \times 10^{+9}$	$2.3382_{-1.5430}^{+1.5430}$	$4.4546_{-2.9336}^{+2.9336}$	$3.534_{-2.329}^{+2.329}$
$\frac{dB}{dq^2}(B \rightarrow a_1(\rightarrow \rho_{\perp}\pi)\mu^+\mu^-) \times 10^{+9}$	$5.7096_{-3.7677}^{+3.7677}$	$10.8774_{-7.1634}^{+7.1634}$	$8.629_{-5.687}^{+5.687}$
$A_{\text{FB}}^{a_1}$	$0.0357_{-0.0004}^{+0.0004}$	$0.0075_{-0.0006}^{+0.0006}$	$0.0140_{-0.0006}^{+0.0006}$
$f_L^{a_1}$	$0.9479_{-0.0008}^{+0.0008}$	$0.9533_{-0.0062}^{+0.0062}$	$0.9492_{-0.0011}^{+0.0011}$

Table 9: Same as in Table 7, but for $q^2 = 2.0 - 3.0 \text{ GeV}^2$ bin.

$q^2 = 2.0 - 3.0 \text{ GeV}^2$			
Observables	SM	Z' Scenario 1	Z' Scenario 2
$\frac{dB}{dq^2}(B \rightarrow \rho\mu^+\mu^-) \times 10^{+9}$	$0.789^{+0.146}_{-0.146}$	$1.443^{+0.266}_{-0.266}$	$1.147^{+0.212}_{-0.212}$
$\frac{dB}{dq^2}(B \rightarrow \rho(\rightarrow \pi\pi)\mu^+\mu^-) \times 10^{+9}$	$0.789^{+0.146}_{-0.146}$	$1.443^{+0.266}_{-0.266}$	$1.147^{+0.212}_{-0.212}$
A_{FB}^ρ	$0.048^{+0.002}_{-0.002}$	$0.033^{+0.001}_{-0.001}$	$0.019^{+0.001}_{-0.001}$
f_L^ρ	$0.880^{+0.001}_{-0.001}$	$0.949^{+0.000}_{-0.000}$	$0.942^{+0.000}_{-0.000}$
$\frac{dB}{dq^2}(B \rightarrow a_1\mu^+\mu^-) \times 10^{+9}$	$7.5818^{+4.9957}_{-4.9957}$	$14.6876^{+9.6632}_{-9.6632}$	$11.570^{+7.618}_{-7.618}$
$\frac{dB}{dq^2}(B \rightarrow a_1(\rightarrow \rho_{\parallel}\pi)\mu^+\mu^-) \times 10^{+9}$	$2.1735^{+1.4321}_{-1.4321}$	$4.2105^{+2.7701}_{-2.7701}$	$3.317^{+2.1837}_{-2.1837}$
$\frac{dB}{dq^2}(B \rightarrow a_1(\rightarrow \rho_{\perp}\pi)\mu^+\mu^-) \times 10^{+9}$	$5.3073^{+3.4970}_{-3.4970}$	$10.2813^{+6.7642}_{-6.7642}$	$8.0399^{+5.3320}_{-5.3320}$
$A_{\text{FB}}^{a_1}$	$0.0230^{+0.0014}_{-0.0014}$	$-0.0036^{+0.0012}_{-0.0012}$	$0.0015^{+0.0014}_{-0.0014}$
$f_L^{a_1}$	$0.9484^{+0.0012}_{-0.0012}$	$0.9584^{+0.0088}_{-0.0088}$	$0.9539^{+0.0010}_{-0.0010}$

 Table 10: Same as in Table 7, but for $q^2 = 3.0 - 4.0 \text{ GeV}^2$ bin.

$q^2 = 3.0 - 4.0 \text{ GeV}^2$			
Observables	SM	Z' Scenario 1	Z' Scenario 2
$\frac{dB}{dq^2}(B \rightarrow \rho\mu^+\mu^-) \times 10^{+9}$	$0.797^{+0.143}_{-0.143}$	$1.503^{+0.269}_{-0.269}$	$1.212^{+0.212}_{-0.212}$
$\frac{dB}{dq^2}(B \rightarrow \rho(\rightarrow \pi\pi)\mu^+\mu^-) \times 10^{+9}$	$0.797^{+0.143}_{-0.143}$	$1.503^{+0.269}_{-0.269}$	$1.212^{+0.212}_{-0.212}$
A_{FB}^ρ	$-0.012^{+0.002}_{-0.002}$	$-0.078^{+0.001}_{-0.001}$	$-0.072^{+0.002}_{-0.002}$
f_L^ρ	$0.8501^{+0.0003}_{-0.0003}$	$0.893^{+0.0005}_{-0.0005}$	$0.8931^{+0.0004}_{-0.0004}$
$\frac{dB}{dq^2}(B \rightarrow a_1\mu^+\mu^-) \times 10^{+9}$	$7.2480^{+4.7714}_{-4.7714}$	$14.1509^{+9.3042}_{-9.3042}$	$11.600^{+7.618}_{-7.618}$
$\frac{dB}{dq^2}(B \rightarrow a_1(\rightarrow \rho_{\parallel}\pi)\mu^+\mu^-) \times 10^{+9}$	$2.0778^{+1.3678}_{-1.3678}$	$4.0566^{+2.6672}_{-2.6672}$	$3.184^{+2.090}_{-2.090}$
$\frac{dB}{dq^2}(B \rightarrow a_1(\rightarrow \rho_{\perp}\pi)\mu^+\mu^-) \times 10^{+9}$	$5.0736^{+3.3400}_{-3.3400}$	$9.9056^{+6.5129}_{-6.5129}$	$7.775^{+5.115}_{-5.115}$
$A_{\text{FB}}^{a_1}$	$0.0079^{+0.0023}_{-0.0023}$	$-0.0157^{+0.0017}_{-0.0017}$	$0.0125^{+0.0020}_{-0.0020}$
$f_L^{a_1}$	$0.9264^{+0.0028}_{-0.0028}$	$0.9384^{+0.0093}_{-0.0093}$	$0.9337^{+0.0027}_{-0.0027}$

 Table 11: Same as in Table 7, but for $q^2 = 4.0 - 5.0 \text{ GeV}^2$ bin.

$q^2 = 4.0 - 5.0 \text{ GeV}^2$			
Observables	SM	Z' Scenario 1	Z' Scenario 2
$\frac{dB}{dq^2}(B \rightarrow \rho\mu^+\mu^-) \times 10^{+9}$	$0.828^{+0.144}_{-0.144}$	$1.587^{+0.276}_{-0.276}$	$1.242^{+0.216}_{-0.216}$
$\frac{dB}{dq^2}(B \rightarrow \rho(\rightarrow \pi\pi)\mu^+\mu^-) \times 10^{+9}$	$0.828^{+0.144}_{-0.144}$	$1.587^{+0.276}_{-0.276}$	$1.242^{+0.216}_{-0.216}$
A_{FB}^ρ	$-0.068^{+0.002}_{-0.002}$	$-0.117^{+0.002}_{-0.002}$	$-0.119^{+0.001}_{-0.001}$
f_L^ρ	$0.8101^{+0.0002}_{-0.0002}$	$0.8315^{+0.0006}_{-0.0006}$	$0.8352^{+0.0005}_{-0.0005}$
$\frac{dB}{dq^2}(B \rightarrow a_1\mu^+\mu^-) \times 10^{+9}$	$6.9869^{+4.5967}_{-4.5967}$	$13.7062^{+9.0082}_{-9.0082}$	$11.110^{+7.307}_{-7.307}$
$\frac{dB}{dq^2}(B \rightarrow a_1(\rightarrow \rho_{\parallel}\pi)\mu^+\mu^-) \times 10^{+9}$	$2.0029^{+1.3177}_{-1.3177}$	$3.9291^{+2.5823}_{-2.5823}$	$3.076^{+2.023}_{-2.023}$
$\frac{dB}{dq^2}(B \rightarrow a_1(\rightarrow \rho_{\perp}\pi)\mu^+\mu^-) \times 10^{+9}$	$4.8908^{+3.2177}_{-3.2177}$	$9.5944^{+6.3057}_{-6.3057}$	$7.512^{+4.939}_{-4.939}$
$A_{\text{FB}}^{a_1}$	$-0.0083^{+0.0031}_{-0.0031}$	$-0.0284^{+0.0022}_{-0.0022}$	$-0.0271^{+0.0026}_{-0.0026}$
$f_L^{a_1}$	$0.8957^{+0.0040}_{-0.0040}$	$0.9087^{+0.0090}_{-0.0090}$	$0.9040^{+0.0040}_{-0.0040}$

Table 12: Same as in Table 7, but for $q^2 = 5.0 - 6.0 \text{ GeV}^2$ bin.

$q^2 = 5.0 - 6.0 \text{ GeV}^2$			
Observables	SM	Z' Scenario 1	Z' Scenario 2
$\frac{dB}{dq^2}(B \rightarrow \rho\mu^+\mu^-) \times 10^{+9}$	$0.868^{+0.147}_{-0.147}$	$1.682^{+0.285}_{-0.285}$	$1.312^{+0.220}_{-0.220}$
$\frac{dB}{dq^2}(B \rightarrow \rho(\rightarrow \pi\pi)\mu^+\mu^-) \times 10^{+9}$	$0.868^{+0.147}_{-0.147}$	$1.682^{+0.285}_{-0.285}$	$1.312^{+0.220}_{-0.220}$
A_{FB}^ρ	$-0.119^{+0.002}_{-0.002}$	$-0.152^{+0.001}_{-0.001}$	$-0.161^{+0.001}_{-0.001}$
f_L^ρ	$0.7601^{+0.0002}_{-0.0002}$	$0.7735^{+0.0006}_{-0.0006}$	$0.7786^{+0.0006}_{-0.0006}$
$\frac{dB}{dq^2}(B \rightarrow a_1\mu^+\mu^-) \times 10^{+9}$	$6.7521^{+4.4407}_{-4.4407}$	$13.2899^{+8.7329}_{-8.7329}$	$10.700^{+7.056}_{-7.056}$
$\frac{dB}{dq^2}(B \rightarrow a_1(\rightarrow \rho_{\parallel}\pi)\mu^+\mu^-) \times 10^{+9}$	$1.9356^{+1.2730}_{-1.2730}$	$3.8098^{+2.5034}_{-2.5034}$	$2.977^{+1.893}_{-1.893}$
$\frac{dB}{dq^2}(B \rightarrow a_1(\rightarrow \rho_{\perp}\pi)\mu^+\mu^-) \times 10^{+9}$	$4.7265^{+3.1085}_{-3.1085}$	$9.3029^{+6.1130}_{-6.1130}$	$7.269^{+4.778}_{-4.778}$
$A_{\text{FB}}^{a_1}$	$-0.0252^{+0.0037}_{-0.0037}$	$-0.0415^{+0.0025}_{-0.0025}$	$-0.0423^{+0.0030}_{-0.0030}$
$f_L^{a_1}$	$0.8599^{+0.0049}_{-0.0049}$	$0.8732^{+0.0084}_{-0.0084}$	$0.8687^{+0.0050}_{-0.0050}$

 Table 13: Same as in Table 7, but for $q^2 = 6.0 - 7.0 \text{ GeV}^2$ bin.

$q^2 = 6.0 - 7.0 \text{ GeV}^2$			
Observables	SM	Z' Scenario 1	Z' Scenario 2
$\frac{dB}{dq^2}(B \rightarrow \rho\mu^+\mu^-) \times 10^{+9}$	$0.912^{+0.150}_{-0.150}$	$1.781^{+0.294}_{-0.294}$	$1.386^{+0.285}_{-0.285}$
$\frac{dB}{dq^2}(B \rightarrow \rho(\rightarrow \pi\pi)\mu^+\mu^-) \times 10^{+9}$	$0.912^{+0.150}_{-0.150}$	$1.781^{+0.294}_{-0.294}$	$1.386^{+0.285}_{-0.285}$
A_{FB}^ρ	$-0.164^{+0.002}_{-0.002}$	$-0.181^{+0.001}_{-0.001}$	$-0.197^{+0.002}_{-0.002}$
f_L^ρ	$0.7101^{+0.0003}_{-0.0003}$	$0.7207^{+0.0006}_{-0.0006}$	$0.7263^{+0.0006}_{-0.0006}$
$\frac{dB}{dq^2}(B \rightarrow a_1\mu^+\mu^-) \times 10^{+9}$	$6.5244^{+4.2905}_{-4.2905}$	$12.8742^{+8.4599}_{-8.4599}$	$10.390^{+6.827}_{-6.827}$
$\frac{dB}{dq^2}(B \rightarrow a_1(\rightarrow \rho_{\parallel}\pi)\mu^+\mu^-) \times 10^{+9}$	$1.8703^{+1.2300}_{-1.2300}$	$3.6906^{+2.4252}_{-2.4252}$	$2.879^{+1.893}_{-1.893}$
$\frac{dB}{dq^2}(B \rightarrow a_1(\rightarrow \rho_{\perp}\pi)\mu^+\mu^-) \times 10^{+9}$	$4.5671^{+3.0034}_{-3.0034}$	$9.0120^{+5.9220}_{-5.9220}$	$7.030^{+4.621}_{-4.621}$
$A_{\text{FB}}^{a_1}$	$-0.0425^{+0.0042}_{-0.0042}$	$-0.0548^{+0.0028}_{-0.0028}$	$-0.0578^{+0.0033}_{-0.0033}$
$f_L^{a_1}$	$0.8204^{+0.0056}_{-0.0056}$	$0.8336^{+0.0076}_{-0.0076}$	$0.8292^{+0.0058}_{-0.0058}$

 Table 14: Same as in Table 7, but for $q^2 = 7.0 - 8.0 \text{ GeV}^2$ bin.

$q^2 = 7.0 - 8.0 \text{ GeV}^2$			
Observables	SM	Z' Scenario 1	Z' Scenario 2
$\frac{dB}{dq^2}(B \rightarrow \rho\mu^+\mu^-) \times 10^{+9}$	$0.959^{+0.150}_{-0.150}$	$1.882^{+0.303}_{-0.303}$	$1.463^{+0.235}_{-0.235}$
$\frac{dB}{dq^2}(B \rightarrow \rho(\rightarrow \pi\pi)\mu^+\mu^-) \times 10^{+9}$	$0.959^{+0.150}_{-0.150}$	$1.882^{+0.303}_{-0.303}$	$1.463^{+0.235}_{-0.235}$
A_{FB}^ρ	$-0.202^{+0.003}_{-0.003}$	$-0.207^{+0.002}_{-0.002}$	$-0.228^{+0.002}_{-0.002}$
f_L^ρ	$0.6602^{+0.0004}_{-0.0004}$	$0.6733^{+0.0006}_{-0.0006}$	$0.6790^{+0.0006}_{-0.0006}$
$\frac{dB}{dq^2}(B \rightarrow a_1\mu^+\mu^-) \times 10^{+9}$	$6.2930^{+4.1389}_{-4.1389}$	$12.4428^{+8.1785}_{-8.1785}$	$10.004^{+6.622}_{-6.622}$
$\frac{dB}{dq^2}(B \rightarrow a_1(\rightarrow \rho_{\parallel}\pi)\mu^+\mu^-) \times 10^{+9}$	$1.8040^{+1.1865}_{-1.1865}$	$3.5669^{+2.3445}_{-2.3445}$	$2.778^{+1.827}_{-1.827}$
$\frac{dB}{dq^2}(B \rightarrow a_1(\rightarrow \rho_{\perp}\pi)\mu^+\mu^-) \times 10^{+9}$	$4.4051^{+2.8972}_{-2.8972}$	$8.7100^{+5.7249}_{-5.7249}$	$6.786^{+4.461}_{-4.461}$
$A_{\text{FB}}^{a_1}$	$-0.0600^{+0.0046}_{-0.0046}$	$-0.0681^{+0.0029}_{-0.0029}$	$-0.0734^{+0.0035}_{-0.0035}$
$f_L^{a_1}$	$0.7778^{+0.0059}_{-0.0059}$	$0.7905^{+0.0068}_{-0.0068}$	$0.7864^{+0.0029}_{-0.0029}$

Table 15: Predictions of averaged values of angular observables for the $B \rightarrow \rho(\rightarrow \pi\pi)\mu^+\mu^-$ decay, in $q^2 = 0.1 - 1.0 \text{ GeV}^2$ bin, for the SM as well as the NP scenarios (S1, S2) of Z' model listed in Table 5. The errors presented mainly come from the uncertainties of the form factors.

$q^2 = 0.1 - 1.0 \text{ GeV}^2$			
Angular Observables	SM	Z' Scenario 1	Z' Scenario 2
$\langle I_{1s}^\rho \rangle$	$0.3524_{-0.0043}^{+0.0043}$	$0.2056_{-0.0039}^{+0.0039}$	$0.2533_{-0.0042}^{+0.0042}$
$\langle I_{1c}^\rho \rangle$	$0.5455_{-0.0060}^{+0.0060}$	$0.7569_{-0.0056}^{+0.0056}$	$0.6882_{-0.0060}^{+0.0060}$
$\langle I_{2s}^\rho \rangle$	$0.0908_{-0.0011}^{+0.0011}$	$0.0517_{-0.0009}^{+0.0009}$	$0.0641_{-0.0011}^{+0.0011}$
$\langle I_{2c}^\rho \rangle$	$-0.4308_{-0.0055}^{+0.0055}$	$-0.4035_{-0.0054}^{+0.0054}$	$-0.4134_{-0.0055}^{+0.0055}$
$\langle I_3^\rho \rangle$	$0.0008_{-0.0003}^{+0.0003}$	$0.0012_{-0.0005}^{+0.0005}$	$0.0012_{-0.0005}^{+0.0005}$
$\langle I_4^\rho \rangle$	$-0.1193_{-0.0003}^{+0.0003}$	$-0.1354_{-0.0003}^{+0.0003}$	$-0.1371_{-0.0003}^{+0.0003}$
$\langle I_5^\rho \rangle$	$0.0024_{-0.0002}^{+0.0002}$	$0.0013_{-0.00005}^{+0.00005}$	$0.0021_{-0.0001}^{+0.0001}$
$\langle I_{6s}^\rho \rangle$	$0.1028_{-0.0003}^{+0.0003}$	$0.0639_{-0.0002}^{+0.0002}$	$0.0918_{-0.0002}^{+0.0002}$
$\langle I_{6c}^\rho \rangle$	0	0	0

Table 16: Same as in Table 15, but for $q^2 = 1.0 - 2.0 \text{ GeV}^2$ bin.

$q^2 = 1.0 - 2.0 \text{ GeV}^2$			
Angular Observables	SM	Z' Scenario 1	Z' Scenario 2
$\langle I_{1s}^\rho \rangle$	$0.1122_{-0.0022}^{+0.0022}$	$0.0238_{-0.0006}^{+0.0006}$	$0.0434_{-0.0011}^{+0.0011}$
$\langle I_{1c}^\rho \rangle$	$0.8629_{-0.0029}^{+0.0029}$	$0.9830_{-0.0008}^{+0.0008}$	$0.9572_{-0.0014}^{+0.0014}$
$\langle I_{2s}^\rho \rangle$	$0.0363_{-0.0007}^{+0.0007}$	$0.0078_{-0.0002}^{+0.0002}$	$0.0139_{-0.0003}^{+0.0003}$
$\langle I_{2c}^\rho \rangle$	$-0.8108_{-0.0031}^{+0.0031}$	$-0.8350_{-0.0033}^{+0.0033}$	$-0.8125_{-0.0032}^{+0.0032}$
$\langle I_3^\rho \rangle$	$-0.0003_{-0.0001}^{+0.0001}$	$0.0013_{-0.0005}^{+0.0005}$	$0.0002_{-0.0001}^{+0.0001}$
$\langle I_4^\rho \rangle$	$-0.0213_{-0.0003}^{+0.0003}$	$-0.0030_{-0.0006}^{+0.0006}$	$-0.0150_{-0.0004}^{+0.0004}$
$\langle I_5^\rho \rangle$	$-0.0124_{-0.0004}^{+0.0004}$	$-0.0037_{-0.0011}^{+0.0011}$	$-0.0090_{-0.0003}^{+0.0003}$
$\langle I_{6s}^\rho \rangle$	$0.1335_{-0.0022}^{+0.0022}$	$0.0863_{-0.0016}^{+0.0016}$	$0.1257_{-0.0020}^{+0.0020}$
$\langle I_{6c}^\rho \rangle$	0	0	0

Table 17: Same as in Table 15, but for $q^2 = 2.0 - 3.0 \text{ GeV}^2$ bin.

$q^2 = 2.0 - 3.0 \text{ GeV}^2$			
Angular Observables	SM	Z' Scenario 1	Z' Scenario 2
$\langle I_{1s}^\rho \rangle$	$0.0854_{-0.0008}^{+0.0008}$	$0.0380_{-0.0002}^{+0.0002}$	$0.0334_{-0.0003}^{+0.0003}$
$\langle I_{1c}^\rho \rangle$	$0.8940_{-0.0011}^{+0.0011}$	$0.9579_{-0.0003}^{+0.0003}$	$0.9506_{-0.0001}^{+0.0001}$
$\langle I_{2s}^\rho \rangle$	$0.0284_{-0.0003}^{+0.0003}$	$0.0125_{-0.0001}^{+0.0001}$	$0.0144_{-0.0001}^{+0.0001}$
$\langle I_{2c}^\rho \rangle$	$-0.8623_{-0.0012}^{+0.0012}$	$-0.9200_{-0.0010}^{+0.0010}$	$-0.8775_{-0.0012}^{+0.0012}$
$\langle I_3^\rho \rangle$	$-0.0032_{-0.0012}^{+0.0012}$	$-0.0032_{-0.0012}^{+0.0012}$	$-0.0029_{-0.0011}^{+0.0011}$
$\langle I_4^\rho \rangle$	$0.0737_{-0.0015}^{+0.0015}$	$0.0941_{-0.0020}^{+0.0020}$	$0.0830_{-0.0018}^{+0.0018}$
$\langle I_5^\rho \rangle$	$-0.0227_{-0.0006}^{+0.0006}$	$-0.0071_{-0.0001}^{+0.0001}$	$-0.0158_{-0.0004}^{+0.0004}$
$\langle I_{6s}^\rho \rangle$	$0.0644_{-0.0025}^{+0.0025}$	$0.0290_{-0.0019}^{+0.0019}$	$0.0612_{-0.0024}^{+0.0024}$
$\langle I_{6c}^\rho \rangle$	0	0	0

Table 18: Same as in Table 15, but for $q^2 = 3.0 - 4.0 \text{ GeV}^2$ bin.

$q^2 = 3.0 - 4.0 \text{ GeV}^2$			
Angular Observables	SM	Z' Scenario 1	Z' Scenario 2
$\langle I_{1s}^\rho \rangle$	$0.1072^{+0.0002}_{-0.0002}$	$0.0804^{+0.0004}_{-0.0004}$	$0.0801^{+0.0003}_{-0.0003}$
$\langle I_{1c}^\rho \rangle$	$0.8624^{+0.0003}_{-0.0003}$	$0.8984^{+0.0005}_{-0.0005}$	$0.8988^{+0.0004}_{-0.0004}$
$\langle I_{2s}^\rho \rangle$	$0.0357^{+0.00009}_{-0.00009}$	$0.0265^{+0.00001}_{-0.00001}$	$0.0266^{+0.00009}_{-0.00009}$
$\langle I_{2c}^\rho \rangle$	$-0.8408^{+0.0004}_{-0.0004}$	$-0.9098^{+0.00008}_{-0.00008}$	$-0.8611^{+0.0003}_{-0.0003}$
$\langle I_3^\rho \rangle$	$-0.0070^{+0.0024}_{-0.0024}$	$-0.0070^{+0.0021}_{-0.0021}$	$-0.0067^{+0.0023}_{-0.0023}$
$\langle I_4^\rho \rangle$	$0.1364^{+0.0025}_{-0.0025}$	$0.1535^{+0.0029}_{-0.0029}$	$0.1452^{+0.0027}_{-0.0027}$
$\langle I_5^\rho \rangle$	$-0.0288^{+0.0007}_{-0.0007}$	$-0.0092^{+0.0002}_{-0.0002}$	$-0.0197^{+0.0004}_{-0.0004}$
$\langle I_{6s}^\rho \rangle$	$-0.0159^{+0.0025}_{-0.0025}$	$-0.0405^{+0.0020}_{-0.0020}$	$-0.0167^{+0.0025}_{-0.0025}$
$\langle I_{6c}^\rho \rangle$	0	0	0

Table 19: Same as in Table 15, but for $q^2 = 4.0 - 5.0 \text{ GeV}^2$ bin.

$q^2 = 4.0 - 5.0 \text{ GeV}^2$			
Angular Observables	SM	Z' Scenario 1	Z' Scenario 2
$\langle I_{1s}^\rho \rangle$	$0.1421^{+0.00002}_{-0.00002}$	$0.1260^{+0.0004}_{-0.0004}$	$0.1235^{+0.0004}_{-0.0004}$
$\langle I_{1c}^\rho \rangle$	$0.8145^{+0.00003}_{-0.00003}$	$0.8356^{+0.0005}_{-0.0005}$	$0.8393^{+0.0005}_{-0.0005}$
$\langle I_{2s}^\rho \rangle$	$0.0473^{+0.000005}_{-0.000005}$	$0.0417^{+0.0001}_{-0.0001}$	$0.0409^{+0.00001}_{-0.00001}$
$\langle I_{2c}^\rho \rangle$	$-0.7987^{+0.00001}_{-0.00001}$	$-0.8690^{+0.0005}_{-0.0005}$	$-0.8202^{+0.0001}_{-0.0001}$
$\langle I_3^\rho \rangle$	$-0.0113^{+0.0036}_{-0.0036}$	$-0.0174^{+0.0030}_{-0.0030}$	$-0.0111^{+0.0035}_{-0.0035}$
$\langle I_4^\rho \rangle$	$0.1786^{+0.0032}_{-0.0032}$	$0.1922^{+0.0035}_{-0.0035}$	$0.1861^{+0.0035}_{-0.0035}$
$\langle I_5^\rho \rangle$	$-0.0323^{+0.0007}_{-0.0007}$	$-0.0106^{+0.0002}_{-0.0002}$	$-0.0219^{+0.0005}_{-0.0005}$
$\langle I_{6s}^\rho \rangle$	$-0.0914^{+0.0026}_{-0.0026}$	$-0.1070^{+0.0020}_{-0.0020}$	$-0.0910^{+0.0025}_{-0.0025}$
$\langle I_{6c}^\rho \rangle$	0	0	0

Table 20: Same as in Table 15, but for $q^2 = 5.0 - 6.0 \text{ GeV}^2$ bin.

$q^2 = 5.0 - 6.0 \text{ GeV}^2$			
Angular Observables	SM	Z' Scenario 1	Z' Scenario 2
$\langle I_{1s}^\rho \rangle$	$0.1792^{+0.0002}_{-0.0002}$	$0.1667^{+0.0004}_{-0.0004}$	$0.1659^{+0.0004}_{-0.0004}$
$\langle I_{1c}^\rho \rangle$	$0.7640^{+0.0002}_{-0.0002}$	$0.7767^{+0.0006}_{-0.0006}$	$0.7818^{+0.0006}_{-0.0006}$
$\langle I_{2s}^\rho \rangle$	$0.0596^{+0.0001}_{-0.0001}$	$0.0561^{+0.0001}_{-0.0001}$	$0.0550^{+0.0001}_{-0.0001}$
$\langle I_{2c}^\rho \rangle$	$-0.7520^{+0.0002}_{-0.0002}$	$-0.8191^{+0.0007}_{-0.0007}$	$-0.7730^{+0.0004}_{-0.0004}$
$\langle I_3^\rho \rangle$	$-0.0163^{+0.0048}_{-0.0048}$	$-0.0164^{+0.0048}_{-0.0049}$	$-0.0161^{+0.0047}_{-0.0047}$
$\langle I_4^\rho \rangle$	$0.2078^{+0.0036}_{-0.0036}$	$0.2185^{+0.0039}_{-0.0039}$	$0.2140^{+0.0031}_{-0.0031}$
$\langle I_5^\rho \rangle$	$-0.0343^{+0.0008}_{-0.0008}$	$-0.0116^{+0.0002}_{-0.0002}$	$-0.0231^{+0.0005}_{-0.0005}$
$\langle I_{6s}^\rho \rangle$	$-0.1589^{+0.0028}_{-0.0028}$	$-0.1668^{+0.0022}_{-0.0022}$	$-0.1578^{+0.0027}_{-0.0027}$
$\langle I_{6c}^\rho \rangle$	0	0	0

Table 21: Same as in Table 15, but for $q^2 = 6.0 - 7.0 \text{ GeV}^2$ bin.

$q^2 = 6.0 - 7.0 \text{ GeV}^2$			
Angular Observables	SM	Z' Scenario 1	Z' Scenario 2
$\langle I_{1s}^\rho \rangle$	$0.2151^{+0.0003}_{-0.0003}$	$0.2093^{+0.0005}_{-0.0005}$	$0.2051^{+0.0005}_{-0.0005}$
$\langle I_{1c}^\rho \rangle$	$0.7156^{+0.0004}_{-0.0004}$	$0.7232^{+0.0006}_{-0.0006}$	$0.7288^{+0.00056}_{-0.0006}$
$\langle I_{2s}^\rho \rangle$	$0.0715^{+0.0001}_{-0.0001}$	$0.0693^{+0.0001}_{-0.0001}$	$0.0680^{+0.0002}_{-0.0002}$
$\langle I_{2c}^\rho \rangle$	$-0.7062^{+0.0004}_{-0.0004}$	$-0.7685^{+0.0009}_{-0.0009}$	$-0.7259^{+0.0005}_{-0.0005}$
$\langle I_3^\rho \rangle$	$-0.0218^{+0.0058}_{-0.0058}$	$-0.0220^{+0.0058}_{-0.0058}$	$-0.0216^{+0.0057}_{-0.0057}$
$\langle I_4^\rho \rangle$	$0.2286^{+0.0040}_{-0.0040}$	$0.2371^{+0.0042}_{-0.0042}$	$0.2338^{+0.0041}_{-0.0041}$
$\langle I_5^\rho \rangle$	$-0.0354^{+0.0008}_{-0.0008}$	$-0.0122^{+0.0003}_{-0.0003}$	$-0.0239^{+0.0006}_{-0.0006}$
$\langle I_{6s}^\rho \rangle$	$-0.2182^{+0.0031}_{-0.0031}$	$-0.2192^{+0.0025}_{-0.0025}$	$-0.2166^{+0.0030}_{-0.0030}$
$\langle I_{6c}^\rho \rangle$	0	0	0

Table 22: Same as in Table 15, but for $q^2 = 7.0 - 8.0 \text{ GeV}^2$ bin.

$q^2 = 7.0 - 8.0 \text{ GeV}^2$			
Angular Observables	SM	Z' Scenario 1	Z' Scenario 2
$\langle I_{1s}^\rho \rangle$	$0.2483^{+0.0003}_{-0.0003}$	$0.2448^{+0.0005}_{-0.0005}$	$0.2406^{+0.0005}_{-0.0005}$
$\langle I_{1c}^\rho \rangle$	$0.6708^{+0.0004}_{-0.0004}$	$0.6753^{+0.0006}_{-0.0006}$	$0.6820^{+0.0007}_{-0.0007}$
$\langle I_{2s}^\rho \rangle$	$0.0826^{+0.0001}_{-0.0001}$	$0.0811^{+0.0002}_{-0.0002}$	$0.0798^{+0.0002}_{-0.0002}$
$\langle I_{2c}^\rho \rangle$	$-0.6632^{+0.0005}_{-0.0005}$	$-0.7230^{+0.0009}_{-0.0009}$	$-0.6815^{+0.0006}_{-0.0006}$
$\langle I_3^\rho \rangle$	$-0.0280^{+0.0068}_{-0.0068}$	$-0.0282^{+0.0065}_{-0.0065}$	$-0.0278^{+0.0067}_{-0.0067}$
$\langle I_4^\rho \rangle$	$0.2437^{+0.0042}_{-0.0042}$	$0.2504^{+0.0044}_{-0.0044}$	$0.2480^{+0.0043}_{-0.0043}$
$\langle I_5^\rho \rangle$	$-0.0357^{+0.0009}_{-0.0009}$	$-0.0126^{+0.0003}_{-0.0003}$	$-0.0239^{+0.0006}_{-0.0006}$
$\langle I_{6s}^\rho \rangle$	$-0.2701^{+0.0035}_{-0.0035}$	$-0.2650^{+0.0029}_{-0.0029}$	$-0.2681^{+0.0034}_{-0.0034}$
$\langle I_{6c}^\rho \rangle$	0	0	0

Table 23: Predictions of averaged values of angular observables for the $B \rightarrow a_1(\rightarrow \rho_{\parallel}\pi)\mu^+\mu^-$ decay, in $q^2 = 0.1 - 1.0 \text{ GeV}^2$ bin, for the SM as well as the NP scenarios (S1, S2) of Z' model listed in Table 5. The errors presented mainly come from the uncertainties of the form factors.

$q^2 = 0.1 - 1.0 \text{ GeV}^2$			
Angular Observables	SM	Z' Scenario 1	Z' Scenario 2
$\langle \widehat{I}_{1s,\parallel}^{a_1} \rangle$	$0.0414^{+0.0007}_{-0.0007}$	$0.0190^{+0.0006}_{-0.0006}$	$0.0251^{+0.0006}_{-0.0006}$
$\langle \widehat{I}_{1c,\parallel}^{a_1} \rangle$	$0.2390^{+0.0009}_{-0.0009}$	$0.2737^{+0.0007}_{-0.0007}$	$0.2643^{+0.0008}_{-0.0008}$
$\langle \widehat{I}_{2s,\parallel}^{a_1} \rangle$	$0.0107^{+0.0002}_{-0.0002}$	$0.0048^{+0.0001}_{-0.0001}$	$0.0064^{+0.0002}_{-0.0002}$
$\langle \widehat{I}_{2c,\parallel}^{a_1} \rangle$	$-0.2027^{+0.0015}_{-0.0015}$	$-0.2211^{+0.0008}_{-0.0008}$	$-0.2159^{+0.0010}_{-0.0010}$
$\langle \widehat{I}_{3,\parallel}^{a_1} \rangle$	$0.0027^{+0.00001}_{-0.00001}$	$0.0024^{+0.00003}_{-0.00003}$	$0.0026^{+0.00002}_{-0.00002}$
$\langle \widehat{I}_{4,\parallel}^{a_1} \rangle$	$-0.0218^{+0.0007}_{-0.0007}$	$-0.0183^{+0.0007}_{-0.0007}$	$-0.0207^{+0.0007}_{-0.0007}$
$\langle \widehat{I}_{5,\parallel}^{a_1} \rangle$	$0.0639^{+0.0002}_{-0.0001}$	$0.0265^{+0.0003}_{-0.0003}$	$0.0366^{+0.0003}_{-0.0003}$
$\langle \widehat{I}_{6s,\parallel}^{a_1} \rangle$	$0.0133^{+0.0002}_{-0.0002}$	$0.0051^{+0.00002}_{-0.00002}$	$0.0073^{+0.0001}_{-0.0001}$
$\langle \widehat{I}_{6c,\parallel}^{a_1} \rangle$	0	0	0

Table 24: Same as in Table 23, but for $q^2 = 1.0 - 2.0 \text{ GeV}^2$ bin.

$q^2 = 1.0 - 2.0 \text{ GeV}^2$			
Angular Observables	SM	Z' Scenario 1	Z' Scenario 2
$\langle \widehat{I}_{1s,\parallel}^{a_1} \rangle$	$0.0112^{+0.0002}_{-0.0002}$	$0.0038^{+0.00003}_{-0.00003}$	$0.0052^{+0.0004}_{-0.0004}$
$\langle \widehat{I}_{1c,\parallel}^{a_1} \rangle$	$0.2743^{+0.0002}_{-0.0002}$	$0.2855^{+0.00007}_{-0.00007}$	$0.2533^{+0.0001}_{-0.0001}$
$\langle \widehat{I}_{2s,\parallel}^{a_1} \rangle$	$0.0036^{+0.00005}_{-0.00005}$	$0.0012^{+0.00001}_{-0.00001}$	$0.0017^{+0.00001}_{-0.00001}$
$\langle \widehat{I}_{2c,\parallel}^{a_1} \rangle$	$-0.2640^{+0.0005}_{-0.0005}$	$-0.2702^{+0.00004}_{-0.00004}$	$-0.2692^{+0.0002}_{-0.0002}$
$\langle \widehat{I}_{3\parallel}^{a_1} \rangle$	$0.0004^{+0.0001}_{-0.0001}$	$-0.0002^{+0.0002}_{-0.0002}$	$0.0016^{+0.0002}_{-0.0002}$
$\langle \widehat{I}_{4\parallel}^{a_1} \rangle$	$0.0103^{+0.0012}_{-0.0012}$	$0.0135^{+0.0011}_{-0.0011}$	$0.0116^{+0.0011}_{-0.0011}$
$\langle \widehat{I}_{5\parallel}^{a_1} \rangle$	$0.0408^{+0.0008}_{-0.0008}$	$0.0124^{+0.0005}_{-0.0005}$	$0.0193^{+0.0007}_{-0.0007}$
$\langle \widehat{I}_{6s,\parallel}^{a_1} \rangle$	$0.0136^{+0.0002}_{-0.0002}$	$0.0029^{+0.0002}_{-0.0002}$	$0.0053^{+0.0002}_{-0.0002}$
$\langle \widehat{I}_{6c,\parallel}^{a_1} \rangle$	0	0	0

Table 25: Same as in Table 23, but for $q^2 = 2.0 - 3.0 \text{ GeV}^2$ bin.

$q^2 = 2.0 - 3.0 \text{ GeV}^2$			
Angular Observables	SM	Z' Scenario 1	Z' Scenario 2
$\langle \widehat{I}_{1s,\parallel}^{a_1} \rangle$	$0.0111^{+0.0003}_{-0.0003}$	$0.0072^{+0.0004}_{-0.0004}$	$0.0076^{+0.0004}_{-0.0004}$
$\langle \widehat{I}_{1c,\parallel}^{a_1} \rangle$	$0.2733^{+0.0004}_{-0.0004}$	$0.2792^{+0.0006}_{-0.0006}$	$0.2786^{+0.0005}_{-0.0005}$
$\langle \widehat{I}_{2s,\parallel}^{a_1} \rangle$	$0.0037^{+0.0001}_{-0.0001}$	$0.0024^{+0.0001}_{-0.0001}$	$0.0025^{+0.0001}_{-0.0001}$
$\langle \widehat{I}_{2c,\parallel}^{a_1} \rangle$	$-0.2675^{+0.0002}_{-0.0002}$	$-0.2705^{+0.0005}_{-0.0005}$	$-0.2705^{+0.0004}_{-0.0004}$
$\langle \widehat{I}_{3\parallel}^{a_1} \rangle$	$-0.0035^{+0.0003}_{-0.0003}$	$-0.0040^{+0.0003}_{-0.0003}$	$-0.0037^{+0.0003}_{-0.0003}$
$\langle \widehat{I}_{4\parallel}^{a_1} \rangle$	$0.0305^{+0.0014}_{-0.0014}$	$0.0329^{+0.0012}_{0.0012}$	$0.0314^{+0.0013}_{-0.0013}$
$\langle \widehat{I}_{5\parallel}^{a_1} \rangle$	$0.0255^{+0.0011}_{-0.0011}$	$0.0043^{+0.0006}_{-0.0006}$	$0.0090^{+0.0007}_{-0.0007}$
$\langle \widehat{I}_{6s,\parallel}^{a_1} \rangle$	$0.0088^{+0.0005}_{-0.0005}$	$-0.0014^{+0.0005}_{-0.0005}$	$0.0001^{+0.0001}_{-0.0001}$
$\langle \widehat{I}_{6c,\parallel}^{a_1} \rangle$	0	0	0

Table 26: Same as in Table 23, but for $q^2 = 3.0 - 4.0 \text{ GeV}^2$ bin.

$q^2 = 3.0 - 4.0 \text{ GeV}^2$			
Angular Observables	SM	Z' Scenario 1	Z' Scenario 2
$\langle \widehat{I}_{1s,\parallel}^{a_1} \rangle$	$0.0158^{+0.0006}_{-0.0006}$	$0.0135^{+0.0007}_{-0.0007}$	$0.0134^{+0.0007}_{-0.0007}$
$\langle \widehat{I}_{1c,\parallel}^{a_1} \rangle$	$0.2666^{+0.0008}_{-0.0008}$	$0.2702^{+0.0010}_{-0.0010}$	$0.2702^{+0.0001}_{-0.0001}$
$\langle \widehat{I}_{2s,\parallel}^{a_1} \rangle$	$0.0053^{+0.0002}_{-0.0002}$	$0.0044^{+0.0002}_{-0.0002}$	$0.0044^{+0.0002}_{-0.0002}$
$\langle \widehat{I}_{2c,\parallel}^{a_1} \rangle$	$-0.2625^{+0.0007}_{-0.0007}$	$-0.2642^{+0.0009}_{-0.0009}$	$-0.2647^{+0.0009}_{-0.0009}$
$\langle \widehat{I}_{3\parallel}^{a_1} \rangle$	$-0.0076^{+0.0004}_{-0.0004}$	$-0.0082^{+0.0004}_{-0.0004}$	$-0.0078^{+0.0003}_{-0.0003}$
$\langle \widehat{I}_{4\parallel}^{a_1} \rangle$	$0.0448^{+0.0014}_{-0.0014}$	$0.0467^{+0.0012}_{-0.0012}$	$0.0455^{+0.0013}_{-0.0013}$
$\langle \widehat{I}_{5\parallel}^{a_1} \rangle$	$0.0155^{+0.0012}_{-0.0012}$	$-0.0011^{+0.0007}_{-0.0007}$	$0.0021^{+0.0008}_{-0.0008}$
$\langle \widehat{I}_{6s,\parallel}^{a_1} \rangle$	$0.0030^{+0.0009}_{-0.0009}$	$0.0060^{+0.0007}_{-0.0007}$	$0.0048^{+0.0008}_{-0.0008}$
$\langle \widehat{I}_{6c,\parallel}^{a_1} \rangle$	0	0	0

Table 27: Same as in Table 23, but for $q^2 = 4.0 - 5.0 \text{ GeV}^2$ bin.

$q^2 = 4.0 - 5.0 \text{ GeV}^2$			
Angular Observables	SM	Z' Scenario 1	Z' Scenario 2
$\langle \widehat{I}_{1s,\parallel}^{a_1} \rangle$	$0.0224_{-0.0009}^{+0.0009}$	$0.0209_{-0.0010}^{+0.0010}$	$0.0206_{-0.0009}^{+0.0009}$
$\langle \widehat{I}_{1c,\parallel}^{a_1} \rangle$	$0.2575_{-0.0012}^{+0.0012}$	$0.2599_{-0.0013}^{+0.0013}$	$0.2603_{-0.0010}^{+0.0010}$
$\langle \widehat{I}_{2s,\parallel}^{a_1} \rangle$	$0.0075_{-0.0003}^{+0.0003}$	$0.0069_{-0.0003}^{+0.0003}$	$0.0068_{-0.0003}^{+0.0003}$
$\langle \widehat{I}_{2c,\parallel}^{a_1} \rangle$	$-0.2545_{-0.0010}^{+0.0010}$	$-0.2554_{-0.0012}^{+0.0012}$	$-0.2561_{-0.0012}^{+0.0012}$
$\langle \widehat{I}_{3\parallel}^{a_1} \rangle$	$-0.0121_{-0.0005}^{+0.0005}$	$-0.0126_{-0.0005}^{+0.0005}$	$-0.0123_{-0.0005}^{+0.0005}$
$\langle \widehat{I}_{4\parallel}^{a_1} \rangle$	$0.0561_{-0.0013}^{+0.0013}$	$0.0576_{-0.0012}^{+0.0012}$	$0.0567_{-0.0012}^{+0.0012}$
$\langle \widehat{I}_{5\parallel}^{a_1} \rangle$	$0.0082_{-0.0013}^{+0.0013}$	$-0.0051_{-0.0007}^{+0.0007}$	$0.0029_{-0.0009}^{+0.0009}$
$\langle \widehat{I}_{6s,\parallel}^{a_1} \rangle$	$-0.0032_{-0.0012}^{+0.0012}$	$-0.0109_{-0.0008}^{+0.0008}$	$-0.0104_{-0.0001}^{+0.0001}$
$\langle \widehat{I}_{6c,\parallel}^{a_1} \rangle$	0	0	0

Table 28: Same as in Table 23, but for $q^2 = 5.0 - 6.0 \text{ GeV}^2$ bin.

$q^2 = 5.0 - 6.0 \text{ GeV}^2$			
Angular Observables	SM	Z' Scenario 1	Z' Scenario 2
$\langle \widehat{I}_{1s,\parallel}^{a_1} \rangle$	$0.0301_{-0.0011}^{+0.0011}$	$0.0291_{-0.0011}^{+0.0011}$	$0.0286_{-0.0013}^{+0.0013}$
$\langle \widehat{I}_{1c,\parallel}^{a_1} \rangle$	$0.2471_{-0.0014}^{+0.0014}$	$0.2487_{-0.0015}^{+0.0015}$	$0.2493_{-0.0015}^{+0.0015}$
$\langle \widehat{I}_{2s,\parallel}^{a_1} \rangle$	$0.0100_{-0.0004}^{+0.0004}$	$0.0096_{-0.0004}^{+0.0004}$	$0.0095_{-0.0038}^{+0.0038}$
$\langle \widehat{I}_{2c,\parallel}^{a_1} \rangle$	$-0.2448_{-0.0013}^{+0.0013}$	$-0.2452_{-0.0015}^{+0.0015}$	$-0.2460_{-0.0015}^{+0.0015}$
$\langle \widehat{I}_{3\parallel}^{a_1} \rangle$	$-0.0169_{-0.0006}^{+0.0006}$	$-0.0174_{-0.0006}^{+0.0006}$	$-0.0170_{-0.0006}^{+0.0006}$
$\langle \widehat{I}_{4\parallel}^{a_1} \rangle$	$0.0655_{-0.0011}^{+0.0011}$	$0.0666_{-0.0010}^{+0.0010}$	$0.0659_{-0.0011}^{+0.0011}$
$\langle \widehat{I}_{5\parallel}^{a_1} \rangle$	$0.0025_{-0.0013}^{+0.0013}$	$-0.0082_{-0.0007}^{+0.0007}$	$0.0068_{-0.0009}^{+0.0009}$
$\langle \widehat{I}_{6s,\parallel}^{a_1} \rangle$	$-0.0096_{-0.0014}^{+0.0014}$	$-0.0158_{-0.0010}^{+0.0010}$	$-0.0162_{-0.0013}^{+0.0013}$
$\langle \widehat{I}_{6c,\parallel}^{a_1} \rangle$	0	0	0

Table 29: Same as in Table 23, but for $q^2 = 6.0 - 7.0 \text{ GeV}^2$ bin.

$q^2 = 6.0 - 7.0 \text{ GeV}^2$			
Angular Observables	SM	Z' Scenario 1	Z' Scenario 2
$\langle \widehat{I}_{1s,\parallel}^{a_1} \rangle$	$0.0386_{-0.0012}^{+0.0012}$	$0.0379_{-0.0013}^{+0.0013}$	$0.0374_{-0.0013}^{+0.0013}$
$\langle \widehat{I}_{1c,\parallel}^{a_1} \rangle$	$0.2357_{-0.0016}^{+0.0016}$	$0.2368_{-0.0017}^{+0.0017}$	$0.2374_{-0.0017}^{+0.0017}$
$\langle \widehat{I}_{2s,\parallel}^{a_1} \rangle$	$0.0128_{-0.0004}^{+0.0004}$	$0.0125_{-0.0004}^{+0.0004}$	$0.0124_{-0.00004}^{+0.00004}$
$\langle \widehat{I}_{2c,\parallel}^{a_1} \rangle$	$-0.2338_{-0.0015}^{+0.0015}$	$-0.2340_{-0.0017}^{+0.0017}$	$-0.2348_{-0.0016}^{+0.0016}$
$\langle \widehat{I}_{3\parallel}^{a_1} \rangle$	$-0.0220_{-0.0006}^{+0.0006}$	$-0.0224_{-0.0006}^{+0.0006}$	$-0.0221_{-0.0007}^{+0.0007}$
$\langle \widehat{I}_{4,\parallel}^{a_1} \rangle$	$0.0734_{-0.0010}^{+0.0010}$	$0.0743_{-0.0009}^{+0.0009}$	$0.0737_{-0.0012}^{+0.0012}$
$\langle \widehat{I}_{5,\parallel}^{a_1} \rangle$	$-0.0021_{-0.0012}^{+0.0012}$	$-0.0106_{-0.0007}^{+0.0007}$	$-0.0091_{-0.0008}^{+0.0008}$
$\langle \widehat{I}_{6s,\parallel}^{a_1} \rangle$	$-0.0162_{-0.0016}^{+0.0016}$	$-0.0209_{-0.0011}^{+0.0011}$	$-0.0220_{-0.0013}^{+0.0013}$
$\langle \widehat{I}_{6c,\parallel}^{a_1} \rangle$	0	0	0

Table 30: Same as in Table 23, but for $q^2 = 7.0 - 8.0 \text{ GeV}^2$ bin.

$q^2 = 7.0 - 8.0 \text{ GeV}^2$			
Angular Observables	SM	Z' Scenario 1	Z' Scenario 2
$\langle \widehat{I}_{1s,\parallel}^{a_1} \rangle$	$0.0478^{+0.0013}_{-0.0013}$	$0.0201^{+0.0008}_{-0.0008}$	$0.0467^{+0.0013}_{-0.0013}$
$\langle \widehat{I}_{1c,\parallel}^{a_1} \rangle$	$0.2233^{+0.0017}_{-0.0017}$	$0.2241^{+0.0018}_{-0.0018}$	$0.2248^{+0.0018}_{-0.0018}$
$\langle \widehat{I}_{2s,\parallel}^{a_1} \rangle$	$0.0159^{+0.0004}_{-0.0004}$	$0.0157^{+0.0004}_{-0.0004}$	$0.0155^{+0.0004}_{-0.0004}$
$\langle \widehat{I}_{2c,\parallel}^{a_1} \rangle$	$-0.2218^{+0.0016}_{-0.0016}$	$-0.2218^{+0.0017}_{-0.0017}$	$-0.2227^{+0.0018}_{-0.0018}$
$\langle \widehat{I}_{3,\parallel}^{a_1} \rangle$	$-0.0274^{+0.0006}_{-0.0006}$	$-0.0278^{+0.0006}_{-0.0006}$	$-0.0275^{+0.0006}_{-0.0006}$
$\langle \widehat{I}_{4,\parallel}^{a_1} \rangle$	$0.0801^{+0.0008}_{-0.0008}$	$0.0808^{+0.0007}_{-0.0007}$	$0.0804^{+0.0007}_{-0.0007}$
$\langle \widehat{I}_{5,\parallel}^{a_1} \rangle$	$-0.0058^{+0.0012}_{-0.0012}$	$-0.0126^{+0.0006}_{-0.0006}$	$-0.0125^{+0.0008}_{-0.0008}$
$\langle \widehat{I}_{6s,\parallel}^{a_1} \rangle$	$-0.0229^{+0.0017}_{-0.0017}$	$-0.0260^{+0.0011}_{-0.0011}$	$-0.0226^{+0.0017}_{-0.0017}$
$\langle \widehat{I}_{6c,\parallel}^{a_1} \rangle$	0	0	0

Table 31: Predictions of averaged values of angular observables for the $B \rightarrow a_1(\rightarrow \rho_\perp \pi)\mu^+\mu^-$ decay, in $q^2 = 0.1 - 1.0 \text{ GeV}^2$ bin, for the SM as well as the NP scenarios (S1, S2) of Z' model listed in Table 5. The errors presented mainly come from the uncertainties of the form factors.

$q^2 = 0.1 - 1.0 \text{ GeV}^2$			
Angular Observables	SM	Z' Scenario 1	Z' Scenario 2
$\langle \widehat{I}_{1s,\perp}^{a_1} \rangle$	$0.3423^{+0.0002}_{-0.0002}$	$0.3574^{+0.0002}_{-0.0002}$	$0.3533^{+0.0002}_{-0.0002}$
$\langle \widehat{I}_{1c,\perp}^{a_1} \rangle$	$0.1010^{+0.0018}_{-0.0018}$	$0.0465^{+0.0013}_{-0.0013}$	$0.0613^{+0.0092}_{-0.0092}$
$\langle \widehat{I}_{2s,\perp}^{a_1} \rangle$	$-0.2345^{+0.0020}_{-0.0020}$	$-0.2641^{+0.0012}_{-0.0012}$	$-0.2558^{+0.0015}_{-0.0015}$
$\langle \widehat{I}_{2c,\perp}^{a_1} \rangle$	$0.0260^{+0.0005}_{-0.0005}$	$0.0117^{+0.0004}_{-0.0004}$	$0.0156^{+0.0004}_{-0.0004}$
$\langle \widehat{I}_{3,\perp}^{a_1} \rangle$	$0.0008^{+0.0003}_{-0.0003}$	$0.0009^{+0.0003}_{-0.0003}$	$0.0001^{+0.0003}_{-0.0003}$
$\langle \widehat{I}_{4,\perp}^{a_1} \rangle$	$0.0267^{+0.0008}_{-0.0008}$	$0.0224^{+0.0009}_{-0.0009}$	$0.0252^{+0.0009}_{-0.0009}$
$\langle \widehat{I}_{5,\perp}^{a_1} \rangle$	$-0.0780^{+0.0002}_{-0.0002}$	$-0.0324^{+0.0003}_{-0.0003}$	$-0.0447^{+0.0003}_{-0.0003}$
$\langle \widehat{I}_{6s,\perp}^{a_1} \rangle$	$0.0162^{+0.0002}_{-0.0002}$	$0.0063^{+0.0002}_{-0.0002}$	$0.0089^{+0.0001}_{-0.0001}$
$\langle \widehat{I}_{6c,\perp}^{a_1} \rangle$	$0.0324^{+0.0005}_{-0.0005}$	$0.0126^{+0.0005}_{-0.0005}$	$0.0178^{+0.0001}_{-0.0001}$

Table 32: Same as in Table 31, but for $q^2 = 1.0 - 2.0 \text{ GeV}^2$ bin.

$q^2 = 1.0 - 2.0 \text{ GeV}^2$			
Angular Observables	SM	Z' Scenario 1	Z' Scenario 2
$\langle \widehat{I}_{1s,\perp}^{a_1} \rangle$	$0.3486^{+0.0002}_{-0.0002}$	$0.3531^{+0.0005}_{-0.0005}$	$0.3533^{+0.0002}_{-0.0002}$
$\langle \widehat{I}_{1c,\perp}^{a_1} \rangle$	$0.0272^{+0.0004}_{-0.0004}$	$0.0092^{+0.0008}_{-0.0008}$	$0.0126^{+0.0001}_{-0.0001}$
$\langle \widehat{I}_{2s,\perp}^{a_1} \rangle$	$-0.3179^{+0.0007}_{-0.0007}$	$-0.3284^{+0.0003}_{-0.0003}$	$-0.3266^{+0.0002}_{-0.0002}$
$\langle \widehat{I}_{2c,\perp}^{a_1} \rangle$	$0.0088^{+0.0001}_{-0.0001}$	$0.0030^{+0.0003}_{-0.0003}$	$0.0041^{+0.0002}_{-0.0002}$
$\langle \widehat{I}_{3,\perp}^{a_1} \rangle$	$0.0030^{+0.0009}_{-0.0009}$	$0.0031^{+0.0009}_{-0.0009}$	$0.0031^{+0.0008}_{-0.0008}$
$\langle \widehat{I}_{4,\perp}^{a_1} \rangle$	$-0.0126^{+0.0015}_{-0.0015}$	$-0.0165^{+0.0014}_{-0.0014}$	$-0.0141^{+0.0011}_{-0.0011}$
$\langle \widehat{I}_{5,\perp}^{a_1} \rangle$	$-0.0498^{+0.0010}_{-0.0010}$	$-0.0151^{+0.0006}_{-0.0006}$	$-0.0236^{+0.0008}_{-0.0008}$
$\langle \widehat{I}_{6s,\perp}^{a_1} \rangle$	$0.0167^{+0.0002}_{-0.0002}$	$0.0035^{+0.0003}_{-0.0003}$	$0.0065^{+0.0003}_{-0.0003}$
$\langle \widehat{I}_{6c,\perp}^{a_1} \rangle$	$0.0333^{+0.0004}_{-0.0004}$	$0.0070^{+0.0005}_{-0.0005}$	$0.0131^{+0.0006}_{-0.0006}$

Table 33: Same as in Table 31, but for $q^2 = 2.0 - 3.0 \text{ GeV}^2$ bin.

$q^2 = 2.0 - 3.0 \text{ GeV}^2$			
Angular Observables	SM	Z' Scenario 1	Z' Scenario 2
$\langle \widehat{I}_{1s,\perp}^{a_1} \rangle$	$0.3473^{+0.0002}_{-0.0002}$	$0.3497^{+0.0002}_{-0.0002}$	$0.3494^{+0.0002}_{-0.0002}$
$\langle \widehat{I}_{1c,\perp}^{a_1} \rangle$	$0.0271^{+0.0006}_{-0.0006}$	$0.0176^{+0.0010}_{-0.0010}$	$0.0185^{+0.0009}_{-0.0009}$
$\langle \widehat{I}_{2s,\perp}^{a_1} \rangle$	$-0.3220^{+0.0003}_{-0.0003}$	$-0.3274^{+0.0008}_{-0.0008}$	$-0.3272^{+0.0006}_{-0.0006}$
$\langle \widehat{I}_{2c,\perp}^{a_1} \rangle$	$0.0090^{+0.0002}_{-0.0002}$	$0.0058^{+0.0003}_{-0.0003}$	$0.0061^{+0.0003}_{-0.0003}$
$\langle \widehat{I}_{3,\perp}^{a_1} \rangle$	$0.0055^{+0.0001}_{-0.0001}$	$0.0055^{+0.0001}_{-0.0001}$	$0.0055^{+0.0001}_{-0.0001}$
$\langle \widehat{I}_{4,\perp}^{a_1} \rangle$	$-0.0372^{+0.0017}_{-0.0017}$	$-0.0401^{+0.0015}_{-0.0015}$	$-0.0383^{+0.0016}_{-0.0016}$
$\langle \widehat{I}_{5,\perp}^{a_1} \rangle$	$-0.0312^{+0.0013}_{-0.0013}$	$-0.0052^{+0.0008}_{-0.0008}$	$-0.0109^{+0.0009}_{-0.0009}$
$\langle \widehat{I}_{6s,\perp}^{a_1} \rangle$	$0.0107^{+0.0007}_{-0.0007}$	$-0.0017^{+0.0006}_{-0.0006}$	$0.0069^{+0.0006}_{-0.0006}$
$\langle \widehat{I}_{6c,\perp}^{a_1} \rangle$	$0.0215^{+0.0013}_{-0.0013}$	$-0.0034^{+0.0011}_{-0.0011}$	$0.0014^{+0.0013}_{-0.0013}$

Table 34: Same as in Table 31, but for $q^2 = 3.0 - 4.0 \text{ GeV}^2$ bin.

$q^2 = 3.0 - 4.0 \text{ GeV}^2$			
Angular Observables	SM	Z' Scenario 1	Z' Scenario 2
$\langle \widehat{I}_{1s,\perp}^{a_1} \rangle$	$0.3448^{+0.0003}_{-0.0003}$	$0.3463^{+0.0003}_{-0.0003}$	$0.3462^{+0.0003}_{-0.0003}$
$\langle \widehat{I}_{1c,\perp}^{a_1} \rangle$	$0.0386^{+0.0014}_{-0.0014}$	$0.0328^{+0.0018}_{-0.0018}$	$0.0326^{+0.0017}_{-0.0017}$
$\langle \widehat{I}_{2s,\perp}^{a_1} \rangle$	$-0.3141^{+0.0011}_{-0.0011}$	$-0.3172^{+0.0014}_{-0.0014}$	$-0.3178^{+0.0013}_{-0.0013}$
$\langle \widehat{I}_{2c,\perp}^{a_1} \rangle$	$0.0128^{+0.0005}_{-0.0005}$	$0.0108^{+0.0006}_{-0.0006}$	$0.0108^{+0.0005}_{-0.0005}$
$\langle \widehat{I}_{3,\perp}^{a_1} \rangle$	$0.0081^{+0.0002}_{-0.0002}$	$0.0081^{+0.0002}_{-0.0002}$	$0.0081^{+0.0002}_{-0.0002}$
$\langle \widehat{I}_{4,\perp}^{a_1} \rangle$	$-0.0547^{+0.0017}_{-0.0017}$	$-0.0570^{+0.0015}_{-0.0015}$	$-0.0556^{+0.0016}_{-0.0016}$
$\langle \widehat{I}_{5,\perp}^{a_1} \rangle$	$-0.0190^{+0.0015}_{-0.0015}$	$-0.0013^{+0.0009}_{-0.0009}$	$-0.0027^{+0.0011}_{-0.0011}$
$\langle \widehat{I}_{6s,\perp}^{a_1} \rangle$	$0.0037^{+0.0011}_{-0.0011}$	$-0.0073^{+0.0008}_{-0.0008}$	$0.0051^{+0.0009}_{-0.0009}$
$\langle \widehat{I}_{6c,\perp}^{a_1} \rangle$	$0.0074^{+0.0022}_{-0.0022}$	$-0.0147^{+0.0016}_{-0.0016}$	$0.0116^{+0.0019}_{-0.0019}$

Table 35: Same as in Table 31, but for $q^2 = 4.0 - 5.0 \text{ GeV}^2$ bin.

$q^2 = 4.0 - 5.0 \text{ GeV}^2$			
Angular Observables	SM	Z' Scenario 1	Z' Scenario 2
$\langle \widehat{I}_{1s,\perp}^{a_1} \rangle$	$0.3418^{+0.0004}_{-0.0004}$	$0.3428^{+0.0004}_{-0.0004}$	$0.3429^{+0.0005}_{-0.0005}$
$\langle \widehat{I}_{1c,\perp}^{a_1} \rangle$	$0.0548^{+0.0021}_{-0.0021}$	$0.0510^{+0.0024}_{-0.0024}$	$0.0502^{+0.0023}_{-0.0023}$
$\langle \widehat{I}_{2s,\perp}^{a_1} \rangle$	$-0.3017^{+0.0016}_{-0.0016}$	$-0.3034^{+0.0019}_{-0.0019}$	$-0.3044^{+0.0019}_{-0.0019}$
$\langle \widehat{I}_{2c,\perp}^{a_1} \rangle$	$0.0182^{+0.0007}_{-0.0007}$	$0.0168^{+0.0008}_{-0.0008}$	$0.0166^{+0.0008}_{-0.0008}$
$\langle \widehat{I}_{3,\perp}^{a_1} \rangle$	$0.0109^{+0.0002}_{-0.0002}$	$0.0109^{+0.0002}_{-0.0002}$	$0.0109^{+0.0002}_{-0.0002}$
$\langle \widehat{I}_{4,\perp}^{a_1} \rangle$	$-0.0685^{+0.0016}_{-0.0016}$	$-0.0703^{+0.0014}_{-0.0014}$	$-0.0691^{+0.0014}_{-0.0014}$
$\langle \widehat{I}_{5,\perp}^{a_1} \rangle$	$-0.0100^{+0.0015}_{-0.0015}$	$-0.0062^{+0.0009}_{-0.0009}$	$-0.0035^{+0.0011}_{-0.0011}$
$\langle \widehat{I}_{6s,\perp}^{a_1} \rangle$	$-0.0039^{+0.0014}_{-0.0014}$	$-0.0133^{+0.0010}_{-0.0010}$	$-0.0127^{+0.0012}_{-0.0012}$
$\langle \widehat{I}_{6c,\perp}^{a_1} \rangle$	$-0.0078^{+0.0029}_{-0.0029}$	$-0.0265^{+0.0020}_{-0.0020}$	$-0.0253^{+0.0024}_{-0.0024}$

Table 36: Same as in Table 31, but for $q^2 = 5.0 - 6.0 \text{ GeV}^2$ bin.

$q^2 = 5.0 - 6.0 \text{ GeV}^2$			
Angular Observables	SM	Z' Scenario 1	Z' Scenario 2
$\langle \widehat{I}_{1s,\perp}^{a_1} \rangle$	$0.3411^{+0.0005}_{-0.0005}$	$0.3392^{+0.0005}_{-0.0005}$	$0.3394^{+0.0005}_{-0.0005}$
$\langle \widehat{I}_{1c,\perp}^{a_1} \rangle$	$0.0735^{+0.0026}_{-0.0026}$	$0.0710^{+0.0028}_{-0.0028}$	$0.0699^{+0.0028}_{-0.0028}$
$\langle \widehat{I}_{2s,\perp}^{a_1} \rangle$	$-0.2866^{+0.0021}_{-0.0021}$	$-0.2877^{+0.0023}_{-0.0023}$	$-0.2888^{+0.0023}_{-0.0023}$
$\langle \widehat{I}_{2c,\perp}^{a_1} \rangle$	$0.0244^{+0.0009}_{-0.0009}$	$0.0235^{+0.0009}_{-0.0009}$	$0.0314^{+0.0009}_{-0.0009}$
$\langle \widehat{I}_{3,\perp}^{a_1} \rangle$	$0.0139^{+0.0002}_{-0.0002}$	$0.0140^{+0.0002}_{-0.0002}$	$0.0140^{+0.0001}_{-0.0001}$
$\langle \widehat{I}_{4,\perp}^{a_1} \rangle$	$-0.0800^{+0.0014}_{-0.0014}$	$-0.0814^{+0.0013}_{-0.0013}$	$-0.0805^{+0.0013}_{-0.0013}$
$\langle \widehat{I}_{5,\perp}^{a_1} \rangle$	$-0.0030^{+0.0015}_{-0.0015}$	$-0.0100^{+0.0009}_{-0.0009}$	$-0.0083^{+0.0011}_{-0.0011}$
$\langle \widehat{I}_{6s,\perp}^{a_1} \rangle$	$-0.0118^{+0.0017}_{-0.0017}$	$-0.0194^{+0.0012}_{-0.0012}$	$-0.0197^{+0.0014}_{-0.0014}$
$\langle \widehat{I}_{6c,\perp}^{a_1} \rangle$	$-0.0235^{+0.0035}_{-0.0035}$	$-0.0387^{+0.0024}_{-0.0024}$	$-0.0395^{+0.0028}_{-0.0028}$

Table 37: Same as in Table 31, but for $q^2 = 6.0 - 7.0 \text{ GeV}^2$ bin.

$q^2 = 6.0 - 7.0 \text{ GeV}^2$			
Angular Observables	SM	Z' Scenario 1	Z' Scenario 2
$\langle \widehat{I}_{1s,\perp}^{a_1} \rangle$	$0.3348^{+0.0005}_{-0.0005}$	$0.3354^{+0.0005}_{-0.0005}$	$0.3355^{+0.0005}_{-0.0005}$
$\langle \widehat{I}_{1c,\perp}^{a_1} \rangle$	$0.0943^{+0.0029}_{-0.0029}$	$0.0926^{+0.0031}_{-0.0031}$	$0.0699^{+0.0028}_{-0.0028}$
$\langle \widehat{I}_{2s,\perp}^{a_1} \rangle$	$-0.2698^{+0.0023}_{-0.0023}$	$-0.2703^{+0.0025}_{-0.0025}$	$-0.2716^{+0.0025}_{-0.0025}$
$\langle \widehat{I}_{2c,\perp}^{a_1} \rangle$	$0.0313^{+0.0010}_{-0.0010}$	$0.0306^{+0.0010}_{-0.0010}$	$0.0302^{+0.0010}_{-0.0010}$
$\langle \widehat{I}_{3,\perp}^{a_1} \rangle$	$0.0173^{+0.0002}_{-0.0002}$	$0.0173^{+0.0002}_{-0.0002}$	$0.0174^{+0.0002}_{-0.0002}$
$\langle \widehat{I}_{4,\perp}^{a_1} \rangle$	$-0.0896^{+0.0012}_{-0.0012}$	$-0.0907^{+0.0011}_{-0.0011}$	$-0.0174^{+0.0001}_{-0.0013}$
$\langle \widehat{I}_{5,\perp}^{a_1} \rangle$	$-0.0026^{+0.0015}_{-0.0015}$	$-0.0130^{+0.0008}_{-0.0008}$	$-0.0122^{+0.0011}_{-0.0011}$
$\langle \widehat{I}_{6s,\perp}^{a_1} \rangle$	$-0.0198^{+0.0020}_{-0.0020}$	$-0.0256^{+0.0013}_{-0.0013}$	$-0.0270^{+0.0016}_{-0.0016}$
$\langle \widehat{I}_{6c,\perp}^{a_1} \rangle$	$-0.0397^{+0.0039}_{-0.0039}$	$-0.0511^{+0.0026}_{-0.0026}$	$-0.0539^{+0.0031}_{-0.0031}$

Table 38: Same as in Table 31, but for $q^2 = 7.0 - 8.0 \text{ GeV}^2$ bin.

$q^2 = 7.0 - 8.0 \text{ GeV}^2$			
Angular Observables	SM	Z' Scenario 1	Z' Scenario 2
$\langle \widehat{I}_{1s,\perp}^{a_1} \rangle$	$0.3310^{+0.0005}_{-0.0005}$	$0.3314^{+0.0006}_{-0.0006}$	$0.3355^{+0.0005}_{-0.0005}$
$\langle \widehat{I}_{1c,\perp}^{a_1} \rangle$	$0.1166^{+0.0031}_{-0.0031}$	$0.1155^{+0.0032}_{-0.0032}$	$0.1142^{+0.0033}_{-0.0033}$
$\langle \widehat{I}_{2s,\perp}^{a_1} \rangle$	$-0.2514^{+0.0025}_{-0.0025}$	$-0.2517^{+0.0027}_{-0.0027}$	$-0.2529^{+0.0025}_{-0.0025}$
$\langle \widehat{I}_{2c,\perp}^{a_1} \rangle$	$0.0388^{+0.0010}_{-0.0010}$	$0.0383^{+0.0011}_{-0.0011}$	$0.03785^{+0.0011}_{-0.0011}$
$\langle \widehat{I}_{3,\perp}^{a_1} \rangle$	$0.0210^{+0.0002}_{-0.0002}$	$0.0210^{+0.0001}_{-0.0001}$	$0.0211^{+0.0001}_{-0.0001}$
$\langle \widehat{I}_{4,\perp}^{a_1} \rangle$	$-0.0978^{+0.0010}_{-0.0010}$	$-0.0987^{+0.0009}_{-0.0009}$	$-0.0982^{+0.0009}_{-0.0009}$
$\langle \widehat{I}_{5,\perp}^{a_1} \rangle$	$0.0071^{+0.0015}_{-0.0015}$	$0.0153^{+0.0008}_{-0.0008}$	$0.0152^{+0.0001}_{-0.0001}$
$\langle \widehat{I}_{6s,\perp}^{a_1} \rangle$	$-0.0280^{+0.0021}_{-0.0021}$	$-0.0318^{+0.0014}_{-0.0014}$	$-0.0343^{+0.0016}_{-0.0016}$
$\langle \widehat{I}_{6c,\perp}^{a_1} \rangle$	$-0.0560^{+0.0043}_{-0.0043}$	$-0.0636^{+0.0027}_{-0.0027}$	$-0.0685^{+0.0033}_{-0.0033}$

References

- [1] S. L. Glashow, J. Iliopoulos, and L. Maiani, *Weak Interactions with Lepton-Hadron Symmetry*, *Phys. Rev. D* **2** (1970) 1285–1292.
- [2] LHCb Collaboration, R. Aaij et al., *Differential branching fractions and isospin asymmetries of $B \rightarrow K^{(*)}\mu^+\mu^-$ decays*, *JHEP* **06** (2014) 133, [[arXiv:1403.8044](#)].
- [3] LHCb Collaboration, R. Aaij et al., *Differential branching fraction and angular analysis of the decay $B^0 \rightarrow K^{*0}\mu^+\mu^-$* , *JHEP* **08** (2013) 131, [[arXiv:1304.6325](#)].
- [4] LHCb Collaboration, R. Aaij et al., *Measurements of the S-wave fraction in $B^0 \rightarrow K^+\pi^-\mu^+\mu^-$ decays and the $B^0 \rightarrow K^*(892)^0\mu^+\mu^-$ differential branching fraction*, *JHEP* **11** (2016) 047, [[arXiv:1606.04731](#)]. [Erratum: *JHEP* **04**, 142 (2017)].
- [5] LHCb Collaboration, R. Aaij et al., *Differential branching fraction and angular analysis of the decay $B_s^0 \rightarrow \phi\mu^+\mu^-$* , *JHEP* **07** (2013) 084, [[arXiv:1305.2168](#)].
- [6] LHCb Collaboration, R. Aaij et al., *Angular analysis and differential branching fraction of the decay $B_s^0 \rightarrow \phi\mu^+\mu^-$* , *JHEP* **09** (2015) 179, [[arXiv:1506.08777](#)].
- [7] S. Descotes-Genon, J. Matias, M. Ramon, and J. Virto, *Implications from clean observables for the binned analysis of $B \rightarrow K^*\mu^+\mu^-$ at large recoil*, *JHEP* **01** (2013) 048, [[arXiv:1207.2753](#)].
- [8] S. Descotes-Genon, T. Hurth, J. Matias, and J. Virto, *Optimizing the basis of $B \rightarrow K^*l\bar{l}$ observables in the full kinematic range*, *JHEP* **05** (2013) 137, [[arXiv:1303.5794](#)].
- [9] S. Ishaq, F. Munir, and I. Ahmed, *Lepton polarization asymmetries in $B \rightarrow K_1l^+l^-$ decay as a searching tool for new physics*, *JHEP* **07** (2013) 006.
- [10] F. Munir, S. Ishaq, and I. Ahmed, *Polarized forward-backward asymmetries of lepton pair in $B \rightarrow K_1l^+l^-$ decay in the presence of New physics*, *PTEP* **2016** (2016), no. 1 013B02, [[arXiv:1511.07075](#)].
- [11] Z.-R. Huang, M. A. Paracha, I. Ahmed, and C.-D. Lü, *Testing Leptoquark and Z' Models via $B \rightarrow K_1(1270, 1400)\mu^+\mu^-$ Decays*, *Phys. Rev. D* **100** (2019), no. 5 055038, [[arXiv:1812.03491](#)].
- [12] F. Munir Bhutta, Z.-R. Huang, C.-D. Lü, M. A. Paracha, and W. Wang, *New physics in $b \rightarrow s\ell\bar{\ell}$ anomalies and its implications for the complementary neutral current decays*, *Nucl. Phys. B* **979** (2022) 115763, [[arXiv:2009.03588](#)].
- [13] D. Das, B. Kindra, G. Kumar, and N. Mahajan, *$B \rightarrow K_2^*(1430)\ell^+\ell^-$ distributions at large recoil in the Standard Model and beyond*, *Phys. Rev. D* **99** (2019), no. 9 093012, [[arXiv:1812.11803](#)].
- [14] M. K. Mohapatra and A. Giri, *Implications of light Z' on semileptonic $B(B_s) \rightarrow T\{K_2^*(1430)(f_2'(1525))\}\ell^+\ell^-$ decays at large recoil*, *Phys. Rev. D* **104** (2021), no. 9 095012, [[arXiv:2109.12382](#)].
- [15] N. Rajeev, N. Sahoo, and R. Dutta, *Angular analysis of $B_s \rightarrow f_2'(1525)(\rightarrow K^+K^-)\mu^+\mu^-$ decays as a probe to lepton flavor universality violation*, *Phys. Rev. D* **103** (2021), no. 9 095007, [[arXiv:2009.06213](#)].

- [16] R. Dutta, *Model independent analysis of new physics effects on $B_c \rightarrow (D_s, D_s^*) \mu^+ \mu^-$ decay observables*, *Phys. Rev. D* **100** (2019), no. 7 075025, [[arXiv:1906.02412](#)].
- [17] M. K. Mohapatra, N. Rajeev, and R. Dutta, *Combined analysis of $B_c \rightarrow D_s^{(*)} \mu^+ \mu^-$ and $B_c \rightarrow D_s^{(*)} \nu \bar{\nu}$ decays within Z' and leptoquark new physics models*, *Phys. Rev. D* **105** (2022), no. 11 115022, [[arXiv:2108.10106](#)].
- [18] M. Zaki, M. A. Paracha, and F. M. Bhutta, *Footprints of New Physics in the angular distribution of $B_c \rightarrow D_s^*(\rightarrow D_s \gamma, (D_s \pi)) \ell^+ \ell^-$ decays*, *Nucl. Phys. B* **992** (2023) 116236, [[arXiv:2303.01145](#)].
- [19] Y.-S. Li and X. Liu, *Angular distribution of the FCNC process $B_c \rightarrow D_s^*(\rightarrow D_s \pi) \ell^+ \ell^-$* , *Phys. Rev. D* **108** (2023), no. 9 093005, [[arXiv:2309.08191](#)].
- [20] **LHCb** Collaboration, R. Aaij et al., *Test of lepton universality with $B^0 \rightarrow K^{*0} \ell^+ \ell^-$ decays*, *JHEP* **08** (2017) 055, [[arXiv:1705.05802](#)].
- [21] **LHCb** Collaboration, R. Aaij et al., *Search for lepton-universality violation in $B^+ \rightarrow K^+ \ell^+ \ell^-$ decays*, *Phys. Rev. Lett.* **122** (2019), no. 19 191801, [[arXiv:1903.09252](#)].
- [22] **LHCb** Collaboration, R. Aaij et al., *Test of lepton universality in beauty-quark decays*, *Nature Phys.* **18** (2022), no. 3 277–282, [[arXiv:2103.11769](#)].
- [23] **BELLE** Collaboration, S. Choudhury et al., *Test of lepton flavor universality and search for lepton flavor violation in $B \rightarrow K \ell \ell$ decays*, *JHEP* **03** (2021) 105, [[arXiv:1908.01848](#)].
- [24] **Belle** Collaboration, A. Abdesselam et al., *Test of Lepton-Flavor Universality in $B \rightarrow K^* \ell^+ \ell^-$ Decays at Belle*, *Phys. Rev. Lett.* **126** (2021), no. 16 161801, [[arXiv:1904.02440](#)].
- [25] **LHCb** Collaboration, R. Aaij et al., *Test of lepton universality in $b \rightarrow s \ell^+ \ell^-$ decays*, *Phys. Rev. Lett.* **131** (2023), no. 5 051803, [[arXiv:2212.09152](#)].
- [26] **LHCb** Collaboration, R. Aaij et al., *Measurement of lepton universality parameters in $B^+ \rightarrow K^+ \ell^+ \ell^-$ and $B^0 \rightarrow K^{*0} \ell^+ \ell^-$ decays*, *Phys. Rev. D* **108** (2023), no. 3 032002, [[arXiv:2212.09153](#)].
- [27] **LHCb** Collaboration, R. Aaij et al., *Measurement of the ratio of branching fractions $\mathcal{B}(\bar{B}^0 \rightarrow D^{*+} \tau^- \bar{\nu}_\tau) / \mathcal{B}(\bar{B}^0 \rightarrow D^{*+} \mu^- \bar{\nu}_\mu)$* , *Phys. Rev. Lett.* **115** (2015), no. 11 111803, [[arXiv:1506.08614](#)]. [Erratum: *Phys.Rev.Lett.* 115, 159901 (2015)].
- [28] **BaBar** Collaboration, J. P. Lees et al., *Measurement of an Excess of $\bar{B} \rightarrow D^{(*)} \tau^- \bar{\nu}_\tau$ Decays and Implications for Charged Higgs Bosons*, *Phys. Rev. D* **88** (2013), no. 7 072012, [[arXiv:1303.0571](#)].
- [29] **Belle** Collaboration, S. Hirose et al., *Measurement of the τ lepton polarization and $R(D^*)$ in the decay $\bar{B} \rightarrow D^* \tau^- \bar{\nu}_\tau$* , *Phys. Rev. Lett.* **118** (2017), no. 21 211801, [[arXiv:1612.00529](#)].
- [30] **LHCb** Collaboration, R. Aaij et al., *Test of Lepton Flavor Universality by the measurement of the $B^0 \rightarrow D^{*-} \tau^+ \nu_\tau$ branching fraction using three-prong τ decays*, *Phys. Rev. D* **97** (2018), no. 7 072013, [[arXiv:1711.02505](#)].
- [31] HFLAV, <https://hflav.web.cern.ch> (End of 2022 Update), and references therein, .

- [32] **Belle** Collaboration, G. Caria et al., *Measurement of $\mathcal{R}(D)$ and $\mathcal{R}(D^*)$ with a semileptonic tagging method*, *Phys. Rev. Lett.* **124** (2020), no. 16 161803, [[arXiv:1910.05864](#)].
- [33] **LHCb** Collaboration, R. Aaij et al., *First measurement of the differential branching fraction and CP asymmetry of the $B^\pm \rightarrow \pi^\pm \mu^+ \mu^-$ decay*, *JHEP* **10** (2015) 034, [[arXiv:1509.00414](#)].
- [34] **LHCb** Collaboration, R. Aaij et al., *Measurement of the $B_s^0 \rightarrow \mu^+ \mu^-$ decay properties and search for the $B^0 \rightarrow \mu^+ \mu^-$ and $B_s^0 \rightarrow \mu^+ \mu^- \gamma$ decays*, *Phys. Rev. D* **105** (2022), no. 1 012010, [[arXiv:2108.09283](#)].
- [35] **LHCb** Collaboration, R. Aaij et al., *Evidence for the decay $B_S^0 \rightarrow \bar{K}^{*0} \mu^+ \mu^-$* , *JHEP* **07** (2018) 020, [[arXiv:1804.07167](#)].
- [36] M. Misiak et al., *Updated NNLO QCD predictions for the weak radiative B-meson decays*, *Phys. Rev. Lett.* **114** (2015), no. 22 221801, [[arXiv:1503.01789](#)].
- [37] **BaBar** Collaboration, P. del Amo Sanchez et al., *Study of $B \rightarrow X\gamma$ Decays and Determination of $|V_{td}/V_{ts}|$* , *Phys. Rev. D* **82** (2010) 051101, [[arXiv:1005.4087](#)].
- [38] R. Bause, H. Gisbert, M. Golz, and G. Hiller, *Model-independent analysis of $b \rightarrow d$ processes*, *Eur. Phys. J. C* **83** (2023), no. 5 419, [[arXiv:2209.04457](#)].
- [39] D. Du, A. X. El-Khadra, S. Gottlieb, A. S. Kronfeld, J. Laiho, E. Lunghi, R. S. Van de Water, and R. Zhou, *Phenomenology of semileptonic B-meson decays with form factors from lattice QCD*, *Phys. Rev. D* **93** (2016), no. 3 034005, [[arXiv:1510.02349](#)].
- [40] A. Ali, A. Y. Parkhomenko, and A. V. Rusov, *Precise Calculation of the Dilepton Invariant-Mass Spectrum and the Decay Rate in $B^\pm \rightarrow \pi^\pm \mu^+ \mu^-$ in the SM*, *Phys. Rev. D* **89** (2014), no. 9 094021, [[arXiv:1312.2523](#)].
- [41] A. V. Rusov, *Probing New Physics in $b \rightarrow d$ transitions*, *JHEP* **07** (2020) 158, [[arXiv:1911.12819](#)].
- [42] M. A. Paracha, *Investigating family non universal Z' model via semileptonic $B \rightarrow a_1 \ell^+ \ell^-$ decays*, *Phys. Scripta* **95** (2020), no. 10 105304.
- [43] P. Nayek, P. Maji, and S. Sahoo, *Study of semileptonic decays $B \rightarrow \pi l^+ l^-$ and $B \rightarrow \rho l^+ l^-$ in nonuniversal Z' model*, *Phys. Rev. D* **99** (2019), no. 1 013005, [[arXiv:1811.09991](#)].
- [44] S. R. Choudhury and N. Gaur, *SUSY effects on the exclusive semileptonic decays $B \rightarrow \pi \tau^+ \tau^-$ and $B \rightarrow \rho \tau^+ \tau^-$* , *Phys. Rev. D* **66** (2002) 094015, [[hep-ph/0206128](#)].
- [45] T. M. Aliev and M. Savci, *Exclusive $B \rightarrow \pi \ell^+ \ell^-$ and $B \rightarrow \rho \ell^+ \ell^-$ decays in two Higgs doublet model*, *Phys. Rev. D* **60** (1999) 014005, [[hep-ph/9812272](#)].
- [46] A. Bharucha, D. M. Straub, and R. Zwicky, *$B \rightarrow V \ell^+ \ell^-$ in the Standard Model from light-cone sum rules*, *JHEP* **08** (2016) 098, [[arXiv:1503.05534](#)].
- [47] R.-H. Li, C.-D. Lu, and W. Wang, *Transition form factors of B decays into p-wave axial-vector mesons in the perturbative QCD approach*, *Phys. Rev. D* **79** (2009) 034014, [[arXiv:0901.0307](#)].
- [48] G. Buchalla, A. J. Buras, and M. E. Lautenbacher, *Weak decays beyond leading logarithms*, *Rev. Mod. Phys.* **68** (1996) 1125–1144, [[hep-ph/9512380](#)].

- [49] K. G. Chetyrkin, M. Misiak, and M. Munz, *Weak radiative B meson decay beyond leading logarithms*, *Phys. Lett. B* **400** (1997) 206–219, [[hep-ph/9612313](#)]. [Erratum: *Phys.Lett.B* 425, 414 (1998)].
- [50] P. Langacker and M. Plumacher, *Flavor changing effects in theories with a heavy Z' boson with family nonuniversal couplings*, *Phys. Rev. D* **62** (2000) 013006, [[hep-ph/0001204](#)].
- [51] V. Barger, L. L. Everett, J. Jiang, P. Langacker, T. Liu, and C. E. M. Wagner, *b → s Transitions in Family-dependent U(1)' Models*, *JHEP* **12** (2009) 048, [[arXiv:0906.3745](#)].
- [52] J. Erler and P. Langacker, *Indications for an extra neutral gauge boson in electroweak precision data*, *Phys. Rev. Lett.* **84** (2000) 212–215, [[hep-ph/9910315](#)].
- [53] C. Bobeth, M. Misiak, and J. Urban, *Photonic penguins at two loops and m_t dependence of BR[B → X_sl⁺l⁻]*, *Nucl. Phys. B* **574** (2000) 291–330, [[hep-ph/9910220](#)].
- [54] M. Beneke, T. Feldmann, and D. Seidel, *Systematic approach to exclusive B → Vl⁺l⁻, Vγ decays*, *Nucl. Phys.* **B612** (2001) 25–58, [[hep-ph/0106067](#)].
- [55] H. H. Asatrian, H. M. Asatrian, C. Greub, and M. Walker, *Two loop virtual corrections to B → X_sl⁺l⁻ in the standard model*, *Phys. Lett. B* **507** (2001) 162–172, [[hep-ph/0103087](#)].
- [56] H. H. Asatryan, H. M. Asatrian, C. Greub, and M. Walker, *Calculation of two loop virtual corrections to b → sl⁺l⁻ in the standard model*, *Phys. Rev.* **D65** (2002) 074004, [[hep-ph/0109140](#)].
- [57] C. Greub, V. Pilipp, and C. Schupbach, *Analytic calculation of two-loop QCD corrections to b → sl⁺l⁻ in the high q² region*, *JHEP* **12** (2008) 040, [[arXiv:0810.4077](#)].
- [58] A. Arhrib, K. Cheung, C.-W. Chiang, and T.-C. Yuan, *Single top-quark production in flavor-changing Z' models*, *Phys. Rev. D* **73** (2006) 075015, [[hep-ph/0602175](#)].
- [59] K. Cheung, C.-W. Chiang, N. G. Deshpande, and J. Jiang, *Constraints on flavor-changing Z' models by B_s mixing, Z' production, and B_s → μ⁺μ⁻*, *Phys. Lett. B* **652** (2007) 285–291, [[hep-ph/0604223](#)].
- [60] Q. Chang, X.-Q. Li, and Y.-D. Yang, *Constraints on the nonuniversal Z' couplings from B → πK, πK* and ρK Decays*, *JHEP* **05** (2009) 056, [[arXiv:0903.0275](#)].
- [61] A. Faessler, T. Gutsche, M. A. Ivanov, J. G. Korner, and V. E. Lyubovitskij, *The Exclusive rare decays B → K(K*) ℓℓ and B_c → D(D*) ℓℓ in a relativistic quark model*, *Eur. Phys. J. direct* **4** (2002), no. 1 18, [[hep-ph/0205287](#)].
- [62] P. Colangelo, F. De Fazio, and F. Loporco, *Probing New Physics with B̄ → ρ(770) ℓ⁻ν̄_ℓ and B̄ → a₁(1260) ℓ⁻ν̄_ℓ*, *Phys. Rev. D* **100** (2019), no. 7 075037, [[arXiv:1906.07068](#)].
- [63] L. Roca, J. E. Palomar, and E. Oset, *Decay of axial vector mesons into VP and Pγ*, *Phys. Rev. D* **70** (2004) 094006, [[hep-ph/0306188](#)].
- [64] **Particle Data Group** Collaboration, R. L. Workman et al., *Review of Particle Physics*, *PTEP* **2022** (2022) 083C01.
- [65] T. Blake, G. Lanfranchi, and D. M. Straub, *Rare B Decays as Tests of the Standard Model*, *Prog. Part. Nucl. Phys.* **92** (2017) 50–91, [[arXiv:1606.00916](#)].

- [66] Q. Chang, X.-Q. Li, and Y.-D. Yang, *Family Non-universal Z' effects on $\bar{B}_q - B_q$ mixing, $B \rightarrow X_s \mu^+ \mu^-$ and $B_s \rightarrow \mu^+ \mu^-$ Decays*, *JHEP* **02** (2010) 082, [[arXiv:0907.4408](#)].
- [67] M. Bona et al., *New Physics from Flavour*, in *Melbourne Neutrino Theory Workshop (Neutrino 08)*, 6, 2009. [arXiv:0906.0953](#).
- [68] A. Cerri et al., *Report from Working Group 4: Opportunities in Flavour Physics at the HL-LHC and HE-LHC*, *CERN Yellow Rep. Monogr.* **7** (2019) 867–1158, [[arXiv:1812.07638](#)].
- [69] **Belle-II** Collaboration, W. Altmannshofer et al., *The Belle II Physics Book*, *PTEP* **2019** (2019), no. 12 123C01, [[arXiv:1808.10567](#)]. [Erratum: PTEP 2020, 029201 (2020)].
- [70] A. Di Canto and S. Meinel, *Weak Decays of b and c Quarks*, [[arXiv:2208.05403](#)].